Pergamon

Int. J. Solids Structures Vol. 33, No. 6, pp. 761–793, 1996

0020-7683/96 $9.50 + .00

0020-7683(95)00077-1

MODELING ADDED COMPRESSIBILITY OF POROSITY AND THE THERMOMECHANICAL RESPONSE OF WET POROUS ROCK WITH APPLICATION TO MT. HELEN TUFF

M. B. RUBIN,

Faculty of Mechanical Engineering, Technion – Israel Institute of Technology, 32000 Haifa, Israel

D. ELATA and A. V. ATTIA

Earth Sciences Division, Lawrence Livermore National Laboratory, P.O. Box 808, Livermore, CA 94550, U.S.A.

(*Received* 10 *November* 1994; *in revised form* 17 *March* 1995)

Abstract—This paper is concerned with modeling the response of a porous brittle solid whose pores may be dry or partially filled with fluid. A form for the Helmholtz free energy is proposed which incorporates known Mie–Grüneisen constitutive equations for the nonporous solid and for the fluid, and which uses an Einstein formulation with variable specific heat. In addition, a functional form for porosity is postulated which depends on two material constants that control the added elastic compressibility of porosity observed in porous rock. The irreversible process of pore crushing is modeled using compaction and dilation surfaces to determine a scalar internal variable that measures unloaded porosity. Restrictions on constitutive assumptions for the composite of porous solid and fluid are obtained which ensure thermodynamic consistency. Examples show that although the added compressibility of porosity is determined by fitting data for dry Mt. Helen tuff, the predicted responses of saturated and partially saturated tuff agree well with experimental data.

1. INTRODUCTION

This paper presents a thermomechanical constitutive model for the response of a rock-like material which is considered to be a composite of a multiply connected solid matrix whose pores are partially or fully saturated with water. The main objective of any theory for such porous materials is to use separate constitutive equations for the nonporous solid material and the fluid to obtain a combined constitutive equation for the response of the composite of the two materials. Here, specific constitutive equations will be developed which model the full range of response from low pressure at room temperature to high pressure at high temperature. Moreover, the proposed constitutive equations use an Einstein formulation of the Helmholtz free energy with variable specific heat.

In many constitutive models, an elemental volume dv of porous material in the present configuration is decomposed into solid volume dv_s and pore volume dv_p such that

$$dv = dv_s + dv_p, \quad dV = dV_s + dV_p, \tag{1a,b}$$

where dV, dV_s, dV_p are the values of dv, dv_s, dv_p, respectively, in a fixed reference configuration. The porosity ϕ and its reference value Φ are then defined by

$$\phi = \frac{dv_p}{dv}, \quad \Phi = \frac{dV_p}{dV}. \tag{2a,b}$$

Also, the Cauchy stress $\mathbf{T}$ at a material point in the medium can be separated into pressure p and deviatoric stress $\mathbf{T}'$ such that

$$\mathbf{T} = -p\mathbf{I} + \mathbf{T}', \quad \mathbf{T}' \cdot \mathbf{I} = 0, \tag{3a,b}$$

where $\mathbf{I}$ is the unit tensor, $\mathbf{A} \cdot \mathbf{B} = \mathrm{tr}(\mathbf{A}\mathbf{B}^{\mathrm{T}})$ denotes the inner product between two second order tensors $\mathbf{A}$, $\mathbf{B}$, and $\mathbf{T}$ is measured positive in tension.

A constitutive equation for the dynamic compaction of ductile porous materials was developed by Herrmann (1969), which assumed that pressure p is a function of the specific internal energy ε and a measure of distention α defined by

$$\alpha = \frac{1}{1-\phi}. \tag{4}$$

Carroll and Holt (1972a) modified the expression for pressure proposed by Herrmann (1969) and related the pressure p in a dry porous material to the average pressure p_s^* in the solid by the formula

$$p = (1-\phi)p_s^*. \tag{5}$$

Later, Carroll and Holt (1972b) proposed a micromechanical model which considered the porous material to be a spherical shell composed of an incompressible ductile material.

When the pores are not evacuated and the porous material is either partially or fully saturated with a fluid, volumetric compression or expansion can cause changes in both the average solid pressure p_s^* and the pressure p_f of the fluid which occupies the pore space. For this case the pressure p is given by (Carroll, 1980)

$$p = (1-\phi)p_s^* + \phi p_f, \tag{6}$$

instead of by eqn (5). This formula is rigorously derived from the balance of linear momentum by neglecting acceleration and body force terms and assuming that the exterior of the porous medium is loaded by a hydrostatic pressure p and that all pores are loaded by the same pressure p_f. However, the formula (6) does not provide a constitutive equation for the average solid pressure p_s^* or for the porosity ϕ.

Typically, the total relative volume J and the average relative volume J_s of the solid are defined by

$$J = \frac{\mathrm{d}v}{\mathrm{d}V}, \quad J_s = \frac{\mathrm{d}v_s}{\mathrm{d}V_s}, \tag{7a,b}$$

and the expressions (1) and (2) are used to deduce that

$$J_s = \left(\frac{1-\phi}{1-\Phi}\right) J. \tag{8}$$

Then, given a constitutive equation for the response $\hat{p}_s(J_s, \theta)$ of the nonporous solid material as a function of J_s and absolute temperature θ, it is usually assumed that the average pressure p_s^* in the porous solid matrix is the same function of J_s and θ as that describing the nonporous solid, so that

$$p_s^* = \hat{p}_s(J_s, \theta). \tag{9}$$

This assumption (9) ignores the effect of stress concentrations near pores in the solid matrix and seems to predict an elastic response that is too stiff. To remedy this problem, the present work models the added elastic compressibility observed in the porous material by proposing a function for the porosity ϕ of the form

$$\phi = \phi(J, \theta, \phi_0). \tag{10}$$

where ϕ_0 is a history-dependent parameter characterizing the porosity of the solid matrix at zero stress and reference temperature θ_0.

A functional form for eqn (10) is proposed which attempts to model the response of a brittle porous material. In particular, it is assumed that during compression, contact stresses between grains cause the grains to fracture and break up into smaller grains which can be further compacted. Upon unloading it is presumed that some grains lose contact before others, causing an apparent added compressibility of the porous material relative to the response associated with a uniform unloading of all grains. Moreover, it is assumed that hysteretic effects of grain rearrangement are negligible so that isothermal (or adiabatic) hydrostatic unloading and reloading occur on the same curve until additional grains are fractured.

Other theoretical modeling of porous materials has been approached from the point of view of a generalized continuum (Goodman and Cowin, 1972), as well as from the point of view of mixture theory (e.g. Drumheller and Bedford, 1980; Nunziato and Walsh, 1980; Baer and Nunziato, 1986; Drumheller, 1987a,b; Baer, 1988; Embid and Baer, 1992; Eringen, 1994; Li, 1994). For the general case of the mixture theory approach, the fluid is allowed to flow through the porous material and the temperature of each constituent may be different. Here, the partially saturated porous material is considered to be a composite of two materials which are in thermal equilibrium so that both the solid and the fluid have the same temperature θ. Also, for the dynamic applications considered here it is assumed that the fluid does not have time to flow through the porous medium.

A set of constitutive equations for the dynamic compaction of wet porous materials has been developed by Drumheller (1987b) using a simplified version of mixture theory (Drumheller and Bedford, 1980), which assumes no relative motion of the solid and fluid and accounts for different temperatures of the solid and fluid. In contrast with the work of Drumheller (1987b), the present theory proposes an explicit form for the Helmholtz free energy that is compatible with Mie–Grüneisen type constitutive equations for the solid and fluid, and it proposes a different procedure for modeling reversible and irreversible changes in porosity.

Prediction of the fluid pressure in the porous medium is important because the deviatoric stress $\mathbf{T}'$ is usually limited by distortional plasticity, with the yield strength of the porous material being a function of both the pressure p and the fluid pressure p_f. In particular, the simplest assumptions of Terzaghi (Jaeger and Cook, 1976, p. 219) take the yield strength to be a function of the effective pressure p_e, which is defined by

$$p_e = p - p_f. \tag{11}$$

Typically, the yield strength is presumed to be a monotonically increasing function of p_e which asymptotically approaches a constant value for large values of p_e. Consequently, this assumption would suggest that when a wet porous material is compressed the yield strength and the effective pressure p_e can remain low even though the pressures p and p_f are quite high. This means that the response of a wet porous material to dynamic shock compression can be significantly influenced by proper modeling of fluid pressure p_f and effective pressure p_e. However, it will be shown that the prediction of the effective pressure p_e is quite sensitive to errors in the prediction of the porosity ϕ. Also, it will be suggested that at high pressure the yield strength may remain high even though p_e may be small.

The present work uses the thermodynamical procedures of Green and Naghdi (1977, 1978) to develop restrictions on the constitutive assumptions which ensure that the first and second laws of thermodynamics are satisfied. After discussing rather general constitutive equations for an elastically isotropic elastic–plastic response, specific constitutive equations are proposed for the Helmholtz free energy of the composite material, which is assumed to be a mass weighted average of the Helmholtz free energies of the solid and fluid constituents. Within this context, the pressure p of the composite is determined by a derivative of the

Helmholtz free energy which yields a functional form different from eqn (6) [with p_s^* given by eqn (9)] when ϕ in eqn (10) depends on J.

One objective of the present development is to provide a simple theoretical structure that retains sufficient generality to match certain features of experimental data. In this regard, the compaction surface which determines the evolution of ϕ_u is characterized by a function which can be used to match details of experimental data for pressure as a function of the total volume during compaction. For increased flexibility the theoretical structure allows this function to be a piecewise linear function which is specified by tabular data. Also, the constitutive model allows the Mie–Grüneisen form for the pressure of both the solid and the fluid to be determined by tabular data for shock velocity as a function of particle velocity, and Grüneisen gamma as a function of relative volume for each constituent.

The following sections provide a brief review (Section 2) of the thermodynamical procedures proposed by Green and Naghdi (1977, 1978) and then discuss a theoretical structure for general constitutive equations (Section 3). Section 4 presents specific constitutive equations and Section 5 describes the procedure for determining constitutive constants and functions which adequately simulate the experimental data of Heard *et al.* (1973) for dry, partially saturated and fully saturated Mt. Helen tuff. Also, examples are presented in Section 5 which explore the influence of ignoring the added compressibility observed in porous materials and which explore the response to shock loading to high pressure and temperature.

2. THERMODYNAMICAL BACKGROUND

By way of background, let $\mathbf{X}$ denote the location of a material point in the reference configuration and $\mathbf{x}$ denote the location of the same material point in the present configuration at time t. Also, let $\mathbf{F} = \partial \mathbf{x}/\partial \mathbf{X}$ be the deformation gradient and $\mathbf{C} = \mathbf{F}^T\mathbf{F}$ be the total deformation. Following the thermodynamic procedures proposed by Green and Naghdi (1977, 1978) the local form of the balance of entropy may be written as

$$\rho\dot{\eta} = \rho(s+\xi) - \operatorname{div}\mathbf{p}, \tag{12}$$

where ρ is the mass per unit present volume, η is the specific (per unit mass) entropy, s is the specific external rate of supply of entropy, ξ is the specific rate of internal production of entropy, $\mathbf{p}$ is the entropy flux vector per unit present area, a superposed dot denotes material time differentiation holding $\mathbf{X}$ fixed, and div denotes the divergence operator with respect to the present position $\mathbf{x}$. Furthermore, the quantities s and $\mathbf{p}$ are related to the specific rate of heat supply r and the heat flux $\mathbf{q}$ per unit present area, appearing in the balance of energy, by the expressions

$$s = \frac{r}{\theta}, \quad \mathbf{p} = \frac{\mathbf{q}}{\theta}. \tag{13a,b}$$

In general ξ may be separated into two parts

$$\rho\theta\xi = -\mathbf{p}\cdot\mathbf{g} + \rho\theta\xi', \tag{14}$$

where $\mathbf{g} = \partial\theta/\partial\mathbf{x}$ is the temperature gradient with respect to the present configuration, so that eqns (12)–(14) may be used to obtain

$$\rho r - \operatorname{div}\mathbf{q} = \rho\theta\dot{\eta} - \rho\theta\xi'. \tag{15}$$

Also, $\mathbf{p}\cdot\mathbf{g}$ denotes the usual scalar product between two vectors. In their work, Green and Naghdi (1977, 1978) developed restrictions on constitutive equations by requiring the

balances of angular momentum and energy to be identically satisfied for all thermomechanical processes. By using the balance of linear momentum to eliminate the specific body force, and the balance of entropy to eliminate the specific rate of heat supply r, it follows that the balance of energy reduces to

$$\rho(\dot{\psi}+\eta\dot{\theta})-\mathbf{T}\cdot\mathbf{D}+\rho\theta\xi''=0, \tag{16}$$

where ψ is the specific Helmholtz free energy and $\mathbf{D}$ is the symmetric part of the velocity gradient $\mathbf{L}$, such that

$$\psi=\varepsilon-\theta\eta, \quad \mathbf{v}=\dot{\mathbf{x}}. \tag{17a,b}$$

$$\mathbf{L}=\frac{\partial\mathbf{v}}{\partial\mathbf{x}}, \qquad \mathbf{D}=\tfrac{1}{2}(\mathbf{L}+\mathbf{L}^{\mathrm{T}}). \tag{17c,d}$$

Also, ε is the specific internal energy, and the symmetry of the stress ($\mathbf{T}=\mathbf{T}^{\mathrm{T}}$) resulting from the balance of angular momentum has been used to obtain eqn (16).

3. GENERAL CONSTITUTIVE RESPONSE

In this section general constitutive equations are developed which explicitly model a compressible porous solid under applied loads that create significant thermomechanical coupling. The effects of plasticity on the response to distortional and dilatational deformations can be modeled by introducing a positive definite symmetric tensor characterizing plastic deformation $\mathbf{C}_{\mathrm{p}}$, which is determined by an evolution equation for its rate. A large deformation model for soils was developed by Rubin (1990), which used the work of Flory (1961) to define a pure measure $I_{3\mathrm{p}}$ of plastic dilatation and a pure measure $\mathbf{C}'_{\mathrm{p}}$ of plastic distortional deformation by the formulas

$$I_{3\mathrm{p}}=\det\mathbf{C}_{\mathrm{p}}, \quad \mathbf{C}'_{\mathrm{p}}=I_{3\mathrm{p}}^{-1/3}\mathbf{C}_{\mathrm{p}}, \quad \det\mathbf{C}'_{\mathrm{p}}=1. \tag{18a,b,c}$$

In that formulation $I_{3\mathrm{p}}$ modeled the effects of porous compaction instead of the unloaded porosity ϕ_{u} used here.

Alternatively, the work of Eckart (1948), Besseling (1966) and Leonov (1976) shows that a theory of plasticity can be developed without introducing a specific measure of plastic deformation (or strain). Instead of defining elastic deformation in terms of total and plastic deformations and proposing an evolution equation for plastic deformation, this alternative formulation focuses attention on the elastic deformation that causes stress by proposing an evolution equation directly for elastic deformation. Specifically, it has been shown (Rubin and Yarin, 1993; Rubin, 1994a,b) that for an elastically isotropic elastic–plastic material, the relaxation effects of distortional plasticity can be modeled by defining an elastic distortional deformation tensor $\mathbf{B}'_{\mathrm{e}}$ together with an evolution equation for its time rate of change. This is accomplished by using the work of Flory (1961) to define

$$J=\det\mathbf{F}, \quad \mathbf{F}'=J^{-1/3}\mathbf{F}, \quad \det\mathbf{F}'=1, \tag{19a,b,c}$$

and by using the work of Rubin and Chen (1991) to define

$$\mathbf{B}'_{\mathrm{e}}=\mathbf{F}'\mathbf{C}'^{-1}_{\mathrm{p}}\mathbf{F}'^{\mathrm{T}}, \quad \det\mathbf{B}'_{\mathrm{e}}=1. \tag{20a,b}$$

Then, recalling that

$$\dot{\mathbf{F}}=\mathbf{L}\mathbf{F}, \quad \dot{J}=J(\mathbf{D}\cdot\mathbf{I}), \tag{21a,b}$$

$$\dot{\mathbf{C}}'^{-1}_{\mathrm{p}}=-\mathbf{C}'^{-1}_{\mathrm{p}}\dot{\mathbf{C}}'_{\mathrm{p}}\mathbf{C}'^{-1}_{\mathrm{p}}, \tag{21c}$$

it follows by differentiating eqn (20a) that the evolution equation for $\mathbf{B}_e'$ may be written in the form

$$\dot{\mathbf{B}}_e' = \mathbf{L}\mathbf{B}_e' + \mathbf{B}_e'\mathbf{L}^T - \tfrac{2}{3}(\mathbf{D}\cdot\mathbf{I})\mathbf{B}_e' - \Gamma\tilde{\mathbf{A}}. \tag{22}$$

In this alternative formulation the quantity $\Gamma\tilde{\mathbf{A}}$ characterizes the relaxation effects of plasticity on the evolution of elastic distortional deformation. Also, the tensor $\tilde{\mathbf{A}}$ in eqn (22) requires a constitutive equation and is related to the expression for $\dot{\mathbf{C}}_p'$ by the formulas

$$\Gamma\tilde{\mathbf{A}} = \mathbf{B}_e'(\mathbf{F}'^{-T}\dot{\mathbf{C}}_p'\mathbf{F}'^{-1})\mathbf{B}_e', \quad \tilde{\mathbf{A}}\cdot\mathbf{B}_e'^{-1} = 0, \tag{23a,b}$$

where the condition (23b) ensures that $\mathbf{B}_e'$ remains unimodular. Recently, Rubin and Attia (1995) have developed a numerical procedure for integrating evolution equations of the type (22), which is based on the work of Rubin (1989).

For the class of constitutive equations under consideration, the response functions ψ, η, $\mathbf{T}$, $\mathbf{p}$, ξ' are assumed to take the forms

$$\psi = \hat{\psi}(U), \qquad \eta = \hat{\eta}(U), \tag{24a,b}$$

$$\mathbf{T} = \hat{\mathbf{T}}(U, \mathbf{B}_e') - q\mathbf{I}, \quad q = \hat{q}(U, \mathbf{D}), \tag{24c,d}$$

$$\mathbf{p} = \hat{\mathbf{p}}(U, \mathbf{B}_e', \mathbf{g}), \qquad \xi' = \hat{\xi}'(U, \dot{\phi}_u, \Gamma, \mathbf{D}), \tag{24e,f}$$

where U denotes the set of variables

$$U = \{J, \phi_u, \theta, \alpha_1, \alpha_2, \kappa\}, \tag{25}$$

the quantities α_1 and α_2 are scalar measures of elastic distortional deformation defined by

$$\alpha_1 = \mathbf{B}_e'\cdot\mathbf{I}, \quad \alpha_2 = \mathbf{B}_e'\cdot\mathbf{B}_e', \tag{26a,b}$$

κ is a measure of isotropic hardening, q in eqn (24c) models "artificial viscosity" which is typically needed in wave propagation codes to eliminate oscillations near shock fronts, and the tensor $\mathbf{B}_e'$ is included in eqns (24c,d) to account for the tensorial properties of $\mathbf{T}$ and $\mathbf{p}$.

Motivated by the strain-space formulation of plasticity proposed by Naghdi and Trapp (1975), a yield function g for determining plastic distortional deformation, a yield function g_c for determining porous compaction ($\dot{\phi}_u < 0$) and a yield function g_d for determining porous dilation ($\dot{\phi}_u > 0$) are introduced such that

$$g = g(U) \leqslant 0, \quad g_c = g_c(U) \leqslant 0, \quad g_d = g_d(U) \leqslant 0. \tag{27a,b,c}$$

Furthermore, the evolution equation for $\mathbf{B}_e'$ is given by eqn (22) and the evolution equations for κ and ϕ_u are given by

$$\dot{\kappa} = \Gamma K, \quad \dot{\phi}_u = \Gamma_\phi, \tag{28a,b}$$

where K is a function of U; and Γ, Γ_ϕ and the tensor $\tilde{\mathbf{A}}$ in eqn (22) are functions of the forms

$$\Gamma = \Gamma(U, R), \quad \Gamma_\phi = \Gamma_\phi(U, R), \quad \tilde{\mathbf{A}} = \tilde{\mathbf{A}}(U, \mathbf{B}_e'), \tag{29a,b,c}$$

with the rates R being defined by

$$R = \{\dot{J}, \mathbf{L}, \dot{\theta}\}. \tag{29d}$$

Assuming that Γ and Γ_ϕ are homogeneous functions of order one in the rates R, it follows that the evolution equations (22) and (28) characterize rate-independent response.

The scalars Γ and Γ_ϕ are determined by loading and unloading conditions which ensure that yield functions $\{g, g_c, g_d\}$ remain nonpositive. In the present formulation, loading corresponds to nonzero values of either $\dot{\phi}_u$ or $\Gamma\tilde{\mathbf{A}}$. Since porous compaction and dilation are assumed to be mutually exclusive processes, it follows that loading may be caused by porous compaction or dilation ($\dot{\phi}_u \neq 0$), or plastic distortional deformation ($\Gamma\tilde{\mathbf{A}} \neq 0$), or both. Moreover, since one or two yield surfaces may be active at any time, the various possible loading and unloading cases are not standard so they have been recorded in Appendix A.

Now, by substituting eqns (22), (24) and (28) into eqn (16) and multiplying the result by J, it follows that

$$\rho_0\left(\frac{\partial\hat{\psi}}{\partial\theta} + \hat{\eta}\right)\dot{\theta} + \left[J\rho_0\frac{\partial\hat{\psi}}{\partial J}\mathbf{I} + 2\rho_0\frac{\partial\hat{\psi}}{\partial\alpha_1}\{\mathbf{B}_e' - \tfrac{1}{3}(\mathbf{B}_e'\cdot\mathbf{I})\mathbf{I}\} + 4\rho_0\frac{\partial\hat{\psi}}{\partial\alpha_2}\{\mathbf{B}_e'^2 - \tfrac{1}{3}(\mathbf{B}_e'^2\cdot\mathbf{I})\mathbf{I}\} - J\hat{\mathbf{T}}\right]\cdot\mathbf{D}$$
$$+ \rho_0\theta\dot{\xi}' + \Gamma_\phi\left[\rho_0\frac{\partial\hat{\psi}}{\partial\phi_u}\right] - \Gamma\left[\rho_0\frac{\partial\hat{\psi}}{\partial\alpha_1}\mathbf{I} + 2\rho_0\frac{\partial\hat{\psi}}{\partial\alpha_2}\mathbf{B}_e'\right]\cdot\tilde{\mathbf{A}} + qJ(\mathbf{D}\cdot\mathbf{I}) = 0, \tag{30}$$

where use has been made of the conservation of mass,

$$\rho J = \rho_0, \tag{31}$$

between the present value ρ and reference value ρ_0 of the mass density. Restrictions on the constitutive assumptions (24) may be obtained by requiring eqn (30) to be satisfied for all thermomechanical processes. In particular, it follows that

$$\hat{\eta} = -\frac{\partial\hat{\psi}}{\partial\theta}, \quad \hat{\mathbf{T}} = -\hat{p}\mathbf{I} + \mathbf{T}', \quad \hat{p} = -\rho_0\frac{\partial\hat{\psi}}{\partial J}, \tag{32a,b,c}$$

$$J\mathbf{T}' = 2\rho_0\frac{\partial\hat{\psi}}{\partial\alpha_1}\{\mathbf{B}_e' - \tfrac{1}{3}(\mathbf{B}_e'\cdot\mathbf{I})\mathbf{I}\} + 4\rho_0\frac{\partial\hat{\psi}}{\partial\alpha_2}\{\mathbf{B}_e'^2 - \tfrac{1}{3}(\mathbf{B}_e'^2\cdot\mathbf{I})\mathbf{I}\}, \tag{32d}$$

$$\rho_0\theta\dot{\xi}' = -\Gamma_\phi\left[\rho_0\frac{\partial\hat{\psi}}{\partial\phi_u}\right] + \Gamma\left[\rho_0\frac{\partial\hat{\psi}}{\partial\alpha_1}\mathbf{I} + 2\rho_0\frac{\partial\hat{\psi}}{\partial\alpha_2}\mathbf{B}_e'\right]\cdot\tilde{\mathbf{A}} - qJ(\mathbf{D}\cdot\mathbf{I}), \tag{32e}$$

are sufficient conditions for eqn (30) to be satisfied for all thermomechanical processes. Notice that the constitutive equations are hyperelastic because the pressure $\hat{p}$ and deviatoric Cauchy stress $\mathbf{T}'$ are determined by derivatives of the Helmholtz free energy.

In view of eqn (32e) it follows that ξ' characterizes the rate of internal production of entropy due to porous compaction and dilation, plastic distortional deformation, and the effects of shock loading, respectively. Further, in this regard it is recalled (Rubin, 1992) that one statement of the second law of thermodynamics requires

$$\rho_0\theta\dot{\xi}' \geq 0 \tag{33}$$

to be valid for all thermomechanical processes.

For a complete constitutive description an additional constitutive equation for the entropy flux $\mathbf{p}$ must be specified. However, since heat conduction is neglected here this constitutive equation is not supplied.

4. SPECIFIC CONSTITUTIVE EQUATIONS

The purpose of this section is to present a specific set of constitutive equations for a porous solid which is partially or fully saturated with a fluid. This is accomplished within the context of the constitutive theory of Section 3. Specifically, it will be assumed that the Helmholtz free energies of the nonporous solid material and the fluid are known. Then a form for the Helmholtz free energy of the partially saturated porous solid will be proposed in terms of the Helmholtz free energies of the individual constituents.

Motivated by the Einstein form of the Helmholtz free energy for a fluid (Hill, 1960, p. 90) and the work of Rubin (1987) on high compression of metals, it is assumed that the specific Helmholtz free energy ψ_s of the nonporous solid matrix material may be represented in the form

$$\rho_{s0}\psi_s = \rho_{s0}\hat{\psi}_s(J_s, \theta, \alpha_1) = \rho_{s0}\hat{\psi}_{s1}(J_s, \theta) + \tfrac{1}{2}\hat{\mu}_s(J_s, \theta)(\alpha_1 - 3), \tag{34a}$$

$$\hat{\psi}_{s1}(J_s, \theta) = C_s\theta \ln\left[2\sinh\left\{\frac{\theta_s(J_s)}{2\theta}\right\}\right] + \varepsilon_{s0}(J_s) - \theta\eta_{s0}, \tag{34b}$$

where ρ_{s0} is the reference density of the solid, $\hat{\psi}_{s1}$ characterizes the response to dilatational deformation, $\hat{\mu}_s$ characterizes the shear modulus, which may depend on (J_s, θ), C_s is a constant controlling the maximum specific heat, θ_s and ε_{s0} are functions of the relative volume J_s to be determined, and η_{s0} is the constant value of entropy at zero temperature and zero elastic distortional strain ($\alpha_1 = 3$). Using the procedures of Section 2 and taking $J = J_s$, it can be shown that the specific entropy η_s, the specific internal energy ε_s, the Cauchy stress $\mathbf{T}_s$, the pressure p_s and the deviatoric stress $\mathbf{T}'_s$ associated with the nonporous solid response are given by

$$\eta_s = -\frac{\partial\hat{\psi}_s}{\partial\theta} = \eta_{s1}(J_s, \theta) + \eta'_s, \tag{35a}$$

$$\eta_{s1} = -\frac{\partial\hat{\psi}_{s1}}{\partial\theta} = \eta_{s0} + C_s\left[\frac{\theta_s}{2\theta}\coth\left\{\frac{\theta_s}{2\theta}\right\} - \ln\left(2\sinh\left\{\frac{\theta_s}{2\theta}\right\}\right)\right], \tag{35b}$$

$$\rho_{s0}\eta'_s = -\frac{1}{2}\frac{\partial\hat{\mu}_s}{\partial\theta}(\alpha_1 - 3), \tag{35c}$$

$$\varepsilon_s = (\psi_s + \theta\eta_s) = \varepsilon_{s1}(J_s, \theta) + \varepsilon'_s, \tag{35d}$$

$$\varepsilon_{s1} = \frac{C_s\theta_s}{2}\coth\left\{\frac{\theta_s}{2\theta}\right\} + \varepsilon_{s0}, \tag{35e}$$

$$\rho_{s0}\varepsilon'_s = \frac{1}{2}\left[\hat{\mu}_s - \theta\frac{\partial\hat{\mu}_s}{\partial\theta}\right](\alpha_1 - 3), \tag{35f}$$

$$\mathbf{T}_s = -p_s\mathbf{I} + \mathbf{T}'_s, \tag{35g}$$

$$p_s = -\rho_{s0}\frac{\partial\hat{\psi}_s}{\partial J_s} = p_{s1}(J_s, \theta) + p'_s, \tag{35h}$$

$$p_{s1} = -\rho_{s0}\left[\frac{d\varepsilon_{s0}}{dJ_s} + \frac{C_s}{2}\frac{d\theta_s}{dJ_s}\coth\left\{\frac{\theta_s}{2\theta}\right\}\right], \tag{35i}$$

$$p_s' = -\frac{1}{2}\frac{\partial \hat{\mu}_s}{\partial J_s}(\alpha_1 - 3), \tag{35j}$$

$$\mathbf{T}_s' = J_s^{-1}\hat{\mu}_s\{\mathbf{B}_e' - \tfrac{1}{3}(\mathbf{B}_e' \cdot \mathbf{I})\mathbf{I}\}. \tag{35k}$$

For convenience, the value of the constant η_{s0} is determined so that the value of η_s vanishes in the reference configuration with $\{J_s = 1, \theta = \theta_0, \mathbf{B}_e' = \mathbf{I}\}$

$$\theta_s(1) = \theta_{s0}, \tag{36a}$$

$$\eta_{s0} = -C_s\left[\frac{\theta_{s0}}{2\theta_0}\coth\left\{\frac{\theta_{s0}}{2\theta_0}\right\} - \ln\left(2\sinh\left\{\frac{\theta_{s0}}{2\theta_0}\right\}\right)\right], \tag{36b}$$

where the value θ_{s0} is determined by the reference value of the specific heat at constant volume. In this regard, it is noted that the specific heat C_{sv} at constant volume and zero elastic distortional strain ($\mathbf{B}_e' = \mathbf{I}$) becomes

$$C_{sv} = \frac{\partial \varepsilon_{s1}}{\partial \theta} = C_s\left[\frac{\frac{\theta_s}{2\theta}}{\sinh\frac{\theta_s}{2\theta}}\right]^2, \tag{37}$$

which shows that C_s is the maximum value of C_{sv}.

Furthermore, it can be shown by solving eqn (35e) for θ and substituting the result into eqn (35i) that the constitutive equations (35) are consistent with a Mie–Grüneisen equation of the form

$$p_{s1} - p_{sH}(J_s) = \rho_{s0}\frac{\gamma_s(J_s)}{J_s}[\varepsilon_{s1} - \varepsilon_{sH}(J_s)], \tag{38}$$

when θ_s and ε_{s0} satisfy the differential equations

$$\frac{1}{\theta_s}\frac{\mathrm{d}\theta_s}{\mathrm{d}J_s} = -\frac{\gamma_s(J_s)}{J_s}, \tag{39a}$$

$$\frac{\mathrm{d}\varepsilon_{s0}}{\mathrm{d}J_s} + \frac{\gamma_s(J_s)}{J_s}\varepsilon_{s0} = -\frac{p_{sH}}{\rho_{s0}} + \frac{\gamma_s(J_s)}{J_s}\varepsilon_{sH}. \tag{39b}$$

In eqn (38), $\gamma_s(J_s)$ is the Grüneisen gamma, $\varepsilon_{sH}(J_s)$ is the specific internal energy on the Hugoniot, and $p_{sH}(J_s)$ is the pressure on the Hugoniot (neglecting strength effects), all for the nonporous solid constituent. Given functional forms for γ_s, ε_{sH} and p_{sH}, eqns (39) can be integrated subject to the condition (36a) and

$$\varepsilon_{s0}(1) = \varepsilon_{sH}(1) - \frac{C_s\theta_{s0}}{2}\coth\left\{\frac{\theta_{s0}}{2\theta_0}\right\}, \tag{40}$$

which ensures that $p_s = p_{sH}$ and $\varepsilon_s = \varepsilon_{sH}$ in the reference configuration (with $J_s = 1$, $\theta = \theta_0$, $\mathbf{B}_e' = \mathbf{I}$).

Next, the fluid is assumed to be an inviscid fluid with no deviatoric stress so the Helmholtz free energy ψ_f of the fluid is taken to have a form similar to ψ_{s1} in eqn (34b) using the relative volume J_f of the fluid defined by

$$J_f = \frac{dv_f}{dV_f}, \tag{41}$$

where dV_f and dv_f are the elemental volumes of the fluid in the reference and present configurations, respectively. Thus, ψ_f is taken in the form

$$\psi_f = \hat{\psi}_f(J_f, \theta) = C_f\theta \ln\left[2\sinh\left\{\frac{\theta_f(J_f)}{2\theta}\right\}\right] + \varepsilon_{f0}(J_f) - \theta\eta_{f0}, \tag{42}$$

where θ_f and ε_{f0} are functions of the relative volume J_f, C_f is a constant controlling the maximum specific heat, and η_{f0} is the constant value of η_f at zero temperature. Using the procedures of Section 2 and taking $J = J_f$, it can be shown that the specific entropy η_f, the specific internal energy ε_f, the Cauchy stress $\mathbf{T}_f$ and the pressure p_f associated with the fluid response are given by

$$\eta_f = \hat{\eta}_f(J_f, \theta) = -\frac{\partial\hat{\psi}_f}{\partial\theta} = \eta_{f0} + C_f\left[\frac{\theta_f}{2\theta}\coth\left\{\frac{\theta_f}{2\theta}\right\} - \ln\left(2\sinh\left\{\frac{\theta_f}{2\theta}\right\}\right)\right], \tag{43a}$$

$$\varepsilon_f = \hat{\varepsilon}_f(J_f, \theta) = (\hat{\psi}_f + \theta\hat{\eta}_f) = \frac{C_f\theta_f}{2}\coth\left\{\frac{\theta_f}{2\theta}\right\} + \varepsilon_{f0}, \tag{43b}$$

$$\mathbf{T}_f = -p_f\mathbf{I}, \tag{43c}$$

$$p_f = \hat{p}_f(J_f, \theta) = -\rho_{f0}\frac{\partial\hat{\psi}_f}{\partial J_f} = -\rho_{f0}\left[\frac{d\varepsilon_{f0}}{dJ_f} + \frac{C_f}{2}\frac{d\theta_f}{dJ_f}\coth\left\{\frac{\theta_f}{2\theta}\right\}\right], \tag{43d}$$

where ρ_{f0} is the reference density of the fluid. Again, the value η_{f0} is specified so that the entropy η_f vanishes in the reference configuration with

$$\theta_f(1) = \theta_{f0}, \tag{44a}$$

$$\eta_{f0} = -C_f\left[\frac{\theta_{f0}}{2\theta_0}\coth\left\{\frac{\theta_{f0}}{2\theta_0}\right\} - \ln\left(2\sinh\left\{\frac{\theta_{f0}}{2\theta_0}\right\}\right)\right], \tag{44b}$$

where the value θ_{f0} is determined by the reference value of the specific heat at constant volume C_{fv}, which is given by

$$C_{fv} = \frac{\partial\varepsilon_f}{\partial\theta} = C_f\left[\frac{\frac{\theta_f}{2\theta}}{\sinh\frac{\theta_f}{2\theta}}\right]^2. \tag{45}$$

It can also be shown by solving eqn (43b) for θ and substituting the result into eqn (43d) that the constitutive equations (43) are consistent with a Mie–Grüneisen equation of the form

$$p_f - p_{fH}(J_f) = \rho_{f0}\frac{\gamma_f(J_f)}{J_f}[\varepsilon_f - \varepsilon_{fH}(J_f)], \tag{46}$$

when θ_f and ε_{f0} satisfy the differential equations

$$\frac{1}{\theta_f}\frac{d\theta_f}{dJ_f} = -\frac{\gamma_f(J_f)}{J_f}. \tag{47a}$$

$$\frac{d\varepsilon_{f0}}{dJ_f} + \frac{\gamma_f(J_f)}{J_f}\varepsilon_{f0} = -\frac{p_{fH}}{\rho_{f0}} + \frac{\gamma_f(J_f)}{J_f}\varepsilon_{fH}. \tag{47b}$$

In eqn (46), $\gamma_f(J_f)$ is the Grüneisen gamma, $\varepsilon_{fH}(J_f)$ is the specific internal energy on the Hugoniot and $p_{fH}(J_f)$ is the pressure on the Hugoniot, all for the fluid constituent. Given functional forms for γ_f, ε_{fH} and p_{fH}, eqns (47) can be integrated subject to the condition (44a) and

$$\varepsilon_{f0}(1) = \varepsilon_{fH}(1) - \frac{C_f\theta_{f0}}{2}\coth\left\{\frac{\theta_{f0}}{2\theta_0}\right\}. \tag{48}$$

which ensures that $p_f = p_{fH}$ and $\varepsilon_f = \varepsilon_{fH}$ in the reference configuration (with $J_f = 1$, $\theta = \theta_0$).

The constitutive equations (42)–(48) are used to model the response of the fluid when it is compressed. Here, the details of vaporization and vapor pressure of the fluid will be ignored. Consequently, these functions may be modified slightly to ensure that the fluid pressure does not become too negative when the fluid is expanding past its zero pressure volume. To this end, it is convenient to let dV_f be the elemental volume of the fluid in the reference configuration and define the value of saturation S of the pore by

$$S = \frac{dV_f}{dV_p}. \tag{49}$$

If the vapor pressure of the fluid is neglected then the pressure in the fluid vanishes until the pores close sufficiently to cause the solid to compress the fluid. This physical process can be modeled simply by assuming that the fluid fills the pores so that the relative volume of the fluid J_f is given by

$$J_f = \frac{dv_f}{dV_f} = \frac{dv_p}{dV_p} = \left(\frac{\phi}{S\Phi}\right)J. \tag{50}$$

Then the constitutive equation for the fluid can be extended so that the pressure nearly vanishes until J_f reaches the value $F_f(\theta)$, causing zero pressure in eqn (43d)

$$p_f(J_f, \theta) = 0 \quad \text{when} \quad J_f = F_f(\theta). \tag{51}$$

More specifically, it is convenient to introduce an effective relative volume $\hat{J}_f(J_f, \theta)$ defined by

$$\hat{J}_f(J_f, \theta) = J_f \qquad \text{for} \quad J_f \leqslant F_f(\theta), \tag{52a}$$

$$\hat{J}_f(J_f, \theta) = F_f(\theta)\left[1 + b_f \tanh\left\{\frac{J_f - F_f(\theta)}{b_f F_f(\theta)}\right\}\right] \quad \text{for} \quad J_f > F_f(\theta), \tag{52b}$$

where b_f is a positive constant to be specified. This function has the properties that $\hat{J}_f$ and its first derivatives with respect to J_f and θ are continuous at $J_f = F_f(\theta)$. Also, notice from eqn (52b) that $\hat{J}_f$ is bounded above

$$\hat{J}_f \leqslant F_f(\theta)[1 + b_f], \tag{53}$$

so that the value of b_f can be used to limit the value of the effective relative volume $\hat{J}_f(J_f, \theta)$

even when J_f becomes large. This latter property is used to ensure that the pressure in the fluid remains near zero during expansion with $J_f > F_f(\theta)$.

In order to model the response of a partially saturated porous material it is assumed that the solid and fluid have the same temperature θ and that the Helmholtz free energy ψ of the composite is a mass weighted average of the Helmholtz free energies of the solid ψ_s and the fluid ψ_f, so that

$$(\mathrm{d}m)\psi = (\mathrm{d}m_s)\psi_s + (\mathrm{d}m_f)\psi_f, \tag{54}$$

where the element of mass $\mathrm{d}m$ of the partially saturated porous material is related to the elements of mass $\mathrm{d}m_s$ and $\mathrm{d}m_f$ of the solid and fluid, respectively,

$$\mathrm{d}m = \mathrm{d}m_s + \mathrm{d}m_f. \tag{55}$$

Dividing eqn (54) by $\mathrm{d}V$ and using the reference values ρ_0, ρ_{s0}, ρ_{f0} of the partially saturated porous material, the solid and the fluid, respectively,

$$\rho_0 = \frac{\mathrm{d}m}{\mathrm{d}V}, \quad \rho_{s0} = \frac{\mathrm{d}m_s}{\mathrm{d}V_s}, \quad \rho_{f0} = \frac{\mathrm{d}m_f}{\mathrm{d}V_f}, \tag{56a,b,c}$$

it can be shown using eqns (1b), (2b) and (49) that

$$\rho_0 = (1-\Phi)\rho_{s0} + S\Phi\rho_{f0}, \tag{57}$$

and that eqn (54) reduces to

$$\rho_0\psi = (1-\Phi)\rho_{s0}\hat{\psi}_s(J_s, \theta, \alpha_1) + S\Phi\rho_{f0}\hat{\psi}_f(\hat{J}_f, \theta). \tag{58}$$

The form (58) makes the simple assumption that the functional form for the Helmholtz free energy of the porous solid is the same as that for the nonporous solid and that porosity only influences the value of the Helmholtz free energy through the dependence of the relative volume J_s defined in eqn (8). Examination of experimental data on Mt. Helen tuff (Heard *et al.*, 1973) indicates that the magnitude of the bulk modulus of the dry porous material at zero pressure is smaller than would be predicted by the assumption (58) if the porosity remains constant during elastic loading and unloading. In order to model the added elastic compressibility observed in porous materials, it is assumed that the porosity ϕ can change during elastic response and a functional form of the type (10) must be specified.

To this end, let $F_s(\theta)$ be the value of J_s which causes the pressure p_{s1} in eqn (35h, i) to vanish, so that

$$p_{s1}(J_s, \theta) = 0 \quad \text{when} \quad J_s = F_s(\theta), \tag{59}$$

and assume that the reference configuration is stress free with $J_s = 1$ so that $F_s(\theta_0) = 1$. Considering a dry porous material, it is assumed that when $J_s = F_s(\theta)$, both p_{s1} and p vanish. In this specific unloaded state ($\theta = \theta_0$), porosity ϕ is denoted by ϕ_u and the corresponding value of J is denoted by J_u using eqn (8),

$$J_u = \frac{1-\Phi}{1-\phi_u}. \tag{60}$$

For compacted states only ($J < J_u$), the specific functional form of eqn (10) is given by

$$\phi_1(J, \phi_u) = \phi_u\left[1 - \frac{a}{b}\tanh\left\{\frac{b}{\phi_u}(1-\phi_u)(\beta-1)\right\}\right], \quad 0 \leqslant \frac{a}{b} < 1, \tag{61a,b}$$

where the auxiliary parameter β is defined by

$$\beta = \frac{J_u}{J}. \tag{62}$$

the parameters a and b are non-negative material constants that control the added compressibility observed in porous materials, and the condition (61b) ensures that ϕ_1 and ϕ_u have the same sign (since $0 \leqslant \phi_u \leqslant 1$). The functional form (61a) was chosen to have the following properties: as the material is compressed with J decreasing from its unloaded value J_u the porosity ϕ_1 decreases relative to its unloaded value ϕ_u; this decrease in ϕ_1 occurs over a smaller range of J as the material becomes more nonporous and ϕ_u decreases; $\phi_1 = \phi_u$ when $J = J_u$ and $\beta = 1$; and $\phi_1 = 1$ when the material is totally dilated with $\phi_u = 1$. Also, this form of ϕ_1 is chosen so that the parameters a and b may easily be determined from experimental data, as will be demonstrated at the end of this section.

For expanded states ($J > J_u$), it follows from eqns (8) and (59) that the value of porosity $\phi_s(J, \theta)$ associated with zero pressure p_{s1} is given by

$$\phi_s(J, \theta) = 1 - \left(\frac{1-\Phi}{J}\right)F_s(\theta). \tag{63}$$

It is assumed that the solid matrix is rather brittle so that it cannot maintain a significant negative value of pressure without creating substantial increase in porosity. Thus, it is expected that in expanded states ($J > J_u$) the value of solid relative volume J_s will remain close to the value $F_s(\theta)$ as the material dilates. To model both compressed and expanded states, the functional form for porosity is specified by

$$\phi(J, \theta, \phi_u) = \hat{\phi}(\phi_1, \phi_s) = \phi_1 \qquad \text{for} \quad \phi_1 \geqslant \phi_s, \tag{64a}$$

$$\phi(J, \theta, \phi_u) = \hat{\phi}(\phi_1, \phi_s) = \phi_s - b_s(1-\phi_s)\tanh\left[\frac{(\phi_s - \phi_1)}{b_s(1-\phi_s)}\right] \quad \text{for} \quad \phi_1 < \phi_s, \tag{64b}$$

respectively, where b_s is another constant. Now, using eqns (8) and (64b) it follows that during dilation ($\phi_1 < \phi_s$) the relative solid volume J_s is given by

$$J_s = F_s(\theta)\left[1 + b_s\tanh\left\{\frac{(\phi_s - \phi_1)}{b_s(1-\phi_s)}\right\}\right] \leqslant F_s(\theta)[1+b_s] \quad \text{for } \phi_1 < \phi_s, \tag{65}$$

so that the value of b_s can be used to ensure that the value of pressure in the solid remains near zero during expansion ($\phi_1 < \phi_s$), even as J becomes large.

Using the definition (63) it follows that for given values of dilatation J and temperature θ the pressure p_1 will vanish when $\phi = \phi_s$ and $J_s = F_s(\theta)$. Assuming that the porosity is given by eqn (64a), eqn (8) may be rewritten in the form

$$\phi_1 = 1 - \left(\frac{1-\Phi}{J}\right)J_s. \tag{66}$$

Consequently, comparison of eqns (63) and (66) indicates that for these same values of J and θ, the condition $\phi_1 > \phi_s$ is satisfied whenever the solid is in a compressed state [$J_s < F_s(\theta)$

and $p_1 > 0$]. Furthermore, the functional form (64) smooths the transition from the compressed state ($\phi_1 > \phi_s$) to the expanded state ($\phi_1 < \phi_s$), since $\hat{\phi}(\phi_1, \phi_s)$ and its first derivatives with respect to ϕ_1 and ϕ_s are continuous when $\phi_1 = \phi_s$. Also, the functional form (64b) causes the porosity ϕ to increase rapidly as the material is expanded ($\phi_1 < \phi_s$) with J increasing, which simulates loss of contact of pieces of a fractured material.

Now, with the help of eqns (21b), (22), (26a), (34), (35), (42), (43), (52), (63) and (64), the expression (58) for the Helmholtz free energy may be substituted into the energy equation (16) to deduce that

$$J^{-1}\left[-(1-\Phi)\rho_{s0}\eta_s - S\Phi\rho_{f0}\eta_f + J(p_s - p_f^*)\frac{\partial\hat{\phi}}{\partial\phi_s}\frac{\partial\phi_s}{\partial\theta} - S\Phi p_f\frac{\partial\hat{J}_f}{\partial\theta} + \rho_0\hat{\eta}\right]\dot{\theta}$$

$$+\left[-\left\{(1-\phi)p_s + \phi p_f^* - J(p_s - p_f^*)\left(\frac{\partial\hat{\phi}}{\partial\phi_1}\frac{\partial\phi_1}{\partial J} + \frac{\partial\hat{\phi}}{\partial\phi_s}\frac{\partial\phi_s}{\partial J}\right)\right\}\mathbf{I} + (1-\phi)\mathbf{T}_s' - \hat{\mathbf{T}}\right]\cdot\mathbf{D} + \rho\theta\hat{\xi}'$$

$$+\left[(p_s - p_f^*)\frac{\partial\hat{\phi}}{\partial\phi_1}\frac{\partial\phi_1}{\partial\phi_u}\right]\dot{\phi}_u - \tfrac{1}{2}\Gamma(1-\Phi)J^{-1}\hat{\mu}_s(\mathbf{I}\cdot\tilde{\mathbf{A}}) + q(\mathbf{D}\cdot\mathbf{I}) = 0, \quad (67)$$

where the pressure p_f^* in the fluid is defined by

$$p_f^* = p_f\frac{\partial\hat{J}_f}{\partial J_f}. \quad (68)$$

Also, η_f and p_f in eqns (67) and (68) are the functions defined in eqns (43a,d), respectively, with the argument J_f replaced by the function $\hat{J}_f$ so that

$$\eta_f = \hat{\eta}_f(\hat{J}_f, \theta), \quad p_f = \hat{p}_f(\hat{J}_f, \theta). \quad (69a,b)$$

It then follows that sufficient conditions for satisfying (67) for all thermomechanical processes are

$$\rho_0\hat{\eta} = (1-\Phi)\rho_{s0}\eta_s + S\Phi\rho_{f0}\eta_f - J(p_s - p_f^*)\frac{\partial\hat{\phi}}{\partial\phi_s}\frac{\partial\phi_s}{\partial\theta} + S\Phi p_f\frac{\partial\hat{J}_f}{\partial\theta}, \quad (70a)$$

$$\hat{p} = (1-\phi)p_s + \phi p_f^* - J(p_s - p_f^*)\left(\frac{\partial\hat{\phi}}{\partial\phi_1}\frac{\partial\phi_1}{\partial J} + \frac{\partial\hat{\phi}}{\partial\phi_s}\frac{\partial\phi_s}{\partial J}\right), \quad (70b)$$

$$\mathbf{T}' = (1-\phi)\mathbf{T}_s', \quad (70c)$$

$$\rho\theta\xi' = \rho\theta\xi_d' + \rho\theta\xi_\phi' + \rho\theta\xi_q', \quad \rho\theta\xi_d' = \tfrac{1}{2}\Gamma(1-\Phi)J^{-1}\hat{\mu}_s(\mathbf{I}\cdot\tilde{\mathbf{A}}), \quad (70d,e)$$

$$\rho\theta\xi_\phi' = -\left[(p_s - p_f^*)\frac{\partial\hat{\phi}}{\partial\phi_1}\frac{\partial\phi_1}{\partial\phi_u}\right]\dot{\phi}_u, \quad \rho\theta\xi_q' = -q(\mathbf{D}\cdot\mathbf{I}), \quad (70f,g)$$

where $\hat{\mathbf{T}}$ is given by eqn (32b) and ξ_d', ξ_ϕ', ξ_q' characterize rates of internal productions of entropy due to: plastic distortional deformation; changes in the unloaded porosity ϕ_u; and shock loading effects, respectively. Also, the internal energy associated with eqns (58) and (70a) becomes

$$\rho_0\varepsilon = \rho_0(\hat{\psi} - \theta\hat{\eta}) = (1-\Phi)\rho_{s0}\varepsilon_s + S\Phi\rho_{f0}\varepsilon_f - \theta\left[J(p_s - p_f^*)\frac{\partial\hat{\phi}}{\partial\phi_s}\frac{\partial\phi_s}{\partial\theta} - S\Phi p_f\frac{\partial\hat{J}_f}{\partial\theta}\right], \quad (71)$$

where the internal energy ε_f of the fluid is the same function as eqn (43b) with the argument J_f replaced by the function $\hat{J}_f$ given by eqn (52).

Notice from eqns (52a), (64a) and (68) that for compressed states with ($\phi_f > \phi_s$ and $J_f < F_f$) the expression (71) reduces to the simple form

$$\rho_0\varepsilon = (1-\Phi)\rho_{s0}\varepsilon_s + S\Phi\rho_{f0}\varepsilon_f, \quad (72)$$

which represents a mass weighted average of the internal energies of the solid and fluid constituents. Also, under these same conditions the formula (70b) for the pressure becomes

$$p = (1-\phi)p_s + \phi p_f - J(p_s - p_f)\frac{\partial\hat{\phi}}{\partial J}. \quad (73)$$

which retains a dependence on the added elastic compressibility of porosity characterized by $\partial\hat{\phi}/\partial J$ with $\phi = \hat{\phi}(J, \phi_0)$. This latter result is due to the assumption that the Helmholtz free energy, which is substituted in the thermodynamic restriction (32c), is a mass weighted average of the form (58). The more complicated formulas (70b) and (71) apply when either the solid or the fluid is expanded beyond its zero pressure density and the approximate functions (52b) and (64b) are employed. Furthermore, comparison of eqns (6) and (73) indicates that for compressed states the average pressure in the solid $p_s^*$is given by

$$p_s^* = p_s - \frac{J(p_s - p_f)}{(1-\phi)}\frac{\partial\hat{\phi}}{\partial J}. \quad (74)$$

which is influenced by the fluid pressure and the added compressibility of porosity. Notice that when the solid and fluid pressures are equal ($p_s = p_f$) the average pressure $p_s^*$is equal to p_s, which is consistent with a homogeneous pressure field in the solid matrix material.

Next, implications of a statement (33) of the second law of thermodynamics are considered which require ξ' in eqn (70d) to be non-negative. Notice from eqns (35) and (70c) that $\mathbf{B}_e'$ equals the identity tensor $\mathbf{I}$ whenever the deviatoric stress vanishes,

$$\mathbf{B}_e' = \mathbf{I} \quad \text{whenever} \quad \mathbf{T}' = 0. \quad (75)$$

Motivated by the assumption that plastic relaxation effects limit the value of deviatoric stress, the tensor $\tilde{\mathbf{A}}$ is specified in the form

$$\tilde{\mathbf{A}} = \left[\mathbf{B}_e' - \left(\frac{3}{\mathbf{B}_e'\cdot\mathbf{I}}\right)\mathbf{I}\right], \quad (76)$$

which satisfies the restriction (23b) and ensures that plastic relaxation effects cause $\mathbf{B}_e'$ to evolve towards the unit tensor $\mathbf{I}$. Now, since $\mathbf{B}_e'$ is unimodular and positive definite, the invariants of $\mathbf{B}_e'$ may be expressed in terms of its eigenvalues and it may be shown that

$$\mathbf{B}_e'\cdot\mathbf{I} \geq 3, \quad \mathbf{B}_e'^{-1}\cdot\mathbf{I} \geq 3, \quad \tilde{\mathbf{A}}\cdot\mathbf{I} \geq 0. \quad (77a,b,c)$$

Furthermore, since $(1-\Phi)J_s^{-1}\mu^*$ is non-negative and the yield function $g(U)$ in eqn (27a) can be specified so that Γ is non-negative, it follows that the dissipation due to plastic distortional relaxation effects is non-negative for all processes.

$$\rho\theta\xi_{\mathrm{d}}' \geqslant 0. \tag{78}$$

Also, the usual form for q in eqn (70g) is specified so that the dissipation effects of shock loading are non-negative for all processes,

$$\rho\theta\xi_{\mathrm{q}}' \geqslant 0. \tag{79}$$

In order to specify forms for the yield functions for porous compaction g_{c} and dilation g_{d} which ensure that the dissipation due to porosity changes is non-negative for all processes,

$$\rho\theta\xi_{\phi}' \geqslant 0, \tag{80}$$

it is convenient to use eqn (68) and define the effective pressure

$$p_{\mathrm{e}} = \hat{p} - p_{\mathrm{f}}^{*}. \tag{81}$$

Specifically, it will be shown that when a is restricted by the condition

$$a < 1, \tag{82}$$

the restriction (80) on the functional form (70f) prevents porous dilation ($\dot{\phi}_{\mathrm{u}} > 0$) when the effective pressure p_{e} is positive and prevents porous compaction ($\dot{\phi}_{\mathrm{u}} < 0$) when p_{e} is negative. To this end, it is necessary to first show that p_{e} has the same sign as the quantity $(p_{\mathrm{s}} - p_{\mathrm{f}}^{*})$ and then show that the product $(\partial\hat{\phi}/\partial\phi_{\mathrm{l}})(\partial\phi_{\mathrm{l}}/\partial\phi_{\mathrm{u}})$ is positive. Thus, with the help of eqns (60)–(62), (64) and (70b) it can be shown that

$$p_{\mathrm{e}} = \left[1 - \phi_{\mathrm{l}} - J\frac{\partial\phi_{\mathrm{l}}}{\partial J}\right](p_{\mathrm{s}} - p_{\mathrm{f}}^{*}) \quad \text{for} \quad \phi_{\mathrm{l}} \geqslant \phi_{\mathrm{s}}, \tag{83a}$$

$$p_{\mathrm{e}} = \frac{\left[1 - \phi_{\mathrm{l}} - J\dfrac{\partial\phi_{\mathrm{l}}}{\partial J}\right](p_{\mathrm{s}} - p_{\mathrm{f}}^{*})}{\cosh^{2}\left[\dfrac{\phi_{\mathrm{s}} - \phi_{\mathrm{l}}}{b_{\mathrm{s}}(1 - \phi_{\mathrm{s}})}\right]} \quad \text{for} \quad \phi_{\mathrm{l}} < \phi_{\mathrm{s}}, \tag{83b}$$

where

$$1 - \phi_{\mathrm{l}} - J\frac{\partial\phi_{\mathrm{l}}}{\partial J} = 1 - \phi_{\mathrm{u}} + \phi_{\mathrm{u}}\frac{a}{b}\tanh\left[\frac{b}{\phi_{\mathrm{u}}}(1 - \phi_{\mathrm{u}})(\beta - 1)\right] - \frac{a(1 - \phi_{\mathrm{u}})\beta}{\cosh^{2}\left[\dfrac{b}{\phi_{\mathrm{u}}}(1 - \phi_{\mathrm{u}})(\beta - 1)\right]}. \tag{84}$$

Moreover, since eqn (84) is a monotonically increasing function of β, its minimum value occurs when $\beta = 0$, so that

$$1 - \phi_{\mathrm{l}} - J\frac{\partial\phi_{\mathrm{l}}}{\partial J} \geqslant (1 - \phi_{\mathrm{u}})\left[1 - a\frac{\tanh\{b(1 - \phi_{\mathrm{u}})/\phi_{\mathrm{u}}\}}{b(1 - \phi_{\mathrm{u}})/\phi_{\mathrm{u}}}\right] > 0, \tag{85}$$

which is positive since $a < 1$ and $0 < \phi_{\mathrm{u}} < 1$. This proves that p_{e} has the same sign as $(p_{\mathrm{s}} - p_{\mathrm{f}}^{*})$. Next, it can be shown using eqn (64) that $(\partial\hat{\phi}/\partial\phi_{\mathrm{l}})$ is positive, so that it only remains to show that $(\partial\phi_{\mathrm{l}}/\partial\phi_{\mathrm{u}})$ is positive. This is accomplished by using eqns (60)–(62) to deduce that

$$\frac{\partial\hat{\phi}_1}{\partial\phi_u} = 1 - \frac{a}{b}\tanh\left\{\frac{b}{\phi_u}(1-\phi_u)(\beta-1)\right\} + \frac{a\{(1-\phi_u)\beta-1\}/\phi_u}{\cosh^2\left\{\frac{b}{\phi_u}(1-\phi_u)(\beta-1)\right\}}, \tag{86a}$$

$$\frac{\hat{c}}{\hat{c}J}\left(\frac{\hat{c}\hat{\phi}_1}{\partial\phi_u}\right) = \frac{2ab(1-\Phi)}{\phi_u^2 J^2}[(1-\phi_u)\beta-1]\left[\frac{\sinh\left\{\frac{b}{\phi_u}(1-\phi_u)(\beta-1)\right\}}{\cosh^3\left\{\frac{b}{\phi_u}(1-\phi_u)(\beta-1)\right\}}\right], \tag{86b}$$

which indicates that as a function of J the quantity $(\hat{c}\hat{\phi}_1/\partial\phi_u)$ has: a local minima for $J = 0$ with $\beta = \infty$; a local maxima for $J = (1-\Phi)/(1-\phi_u)$ with $\beta = 1$; and a local minima for $J = 1-\Phi$ with $\beta = 1/(1-\phi_u)$. Moreover, it can be shown that

$$\frac{\hat{c}\hat{\phi}_1}{\hat{c}\phi_u} \geqslant \min\left[1-a, 1-\frac{a}{b}\right] > 0. \tag{87}$$

Thus, in view of the restrictions (61b) and (82) it can be seen that the quantity $\partial\phi_1/\partial\phi_u$ will remain positive.

The effect of elastic distortion on compaction and dilation has been considered previously (e.g. Rice and Tracey, 1969; DiMaggio and Sandler, 1971; Gurson, 1977) and is included in the general constitutive equations for compaction and dilation surfaces of the forms (27b,c) which include dependence on α_1 and α_2. However, for simplicity this direct dependence on elastic distortion is neglected here and the restriction (80) on porous compaction and dilation is satisfied by introducing a compaction surface of the form

$$g_c = p_e - h(J_s,\theta)f(\phi) \leqslant 0, \quad f(\phi) \geqslant 0, \tag{88a,b}$$

and a dilation surface of the form

$$g_d = -p_e - h(J_s,\theta)\kappa_d \leqslant 0, \quad \kappa_d > 0, \tag{89a,b}$$

where $f(\phi)$ is a non-negative function which is determined by hydrostatic dry compaction data, κ_d is a positive constant which determines the dilation response, and it is tacitly assumed that p_e is a decreasing function of ϕ_u. Also, $h(J_s,\theta)$ is a positive function which controls the response when the temperature reaches the melt temperature $\theta_{Ms}(J_s)$ of the solid. For simplicity, $h(J_s,\theta)$ is specified by

$$h(J_s,\theta) = 1 \qquad \text{for} \quad \theta < \theta_0, \tag{90a}$$

$$h(J_s,\theta) = h_M + (1-h_M)\left\langle\frac{\theta_{Ms}(J_s)-\theta}{\theta_{Ms}(J_s)-\theta_0}\right\rangle^n \qquad \text{for} \quad \theta \geqslant \theta_0, \tag{90b}$$

where the McAuley brackets are defined by

$$\langle x\rangle = \tfrac{1}{2}(x+|x|). \tag{91}$$

h_M is a small positive constant and n is a non-negative constant.

The forms (88) and (89) were chosen to model the following physical limiting cases: (a) for compaction of a dry material (with vanishing p_f^*) the pressure $p = p_e$ is allowed to become arbitrarily large as ϕ approaches zero, since $f(\phi)$ should become unbounded in this limit; (b) for compaction of a dry material the porosity ϕ is driven to zero as the solid material melts (with $\theta \geqslant \theta_{Ms}$), since $h(J_s,\theta)$ drops to the small positive value of h_M which causes added compaction and domination of the singularity of $f(\phi)$ as ϕ approaches zero;

(c) for compaction of a wet material (with $p_f^* > 0$) the effective pressure p_e approaches the small value $h_M f(\phi)$ as the solid melts (with $\theta \geqslant \theta_{Ms}$), since $f(\phi)$ remains bounded for $\phi > 0$ (this also ensures near pressure equilibrium between the solid and the fluid in this limit); (d) for dilation the magnitude of p_e becomes small as the solid melts. Further, in this regard it is noted that experimental data are not available to provide details of the functional form for $h(J_s, \theta)$, so that eqns (90) merely represent a simple form that causes physically reasonable material response in these various extreme limiting conditions.

For the examples considered in the next section on hydrostatic loading, it is not necessary to specify a specific functional form for the yield surface g in eqn (27a) which limits the amount of distortional elastic deformation by plasticity. Nevertheless, for any specified functional forms for the yield, compaction and dilation surfaces it is possible to determine expressions for Γ in eqns (22) and (28a) and Γ_ϕ in eqn (28b) by loading/unloading conditions, as discussed in Appendix A.

To complete the constitutive theory it is necessary to specify a functional form for the solid shear modulus $\hat{\mu}_s$ in eqn (34a). To this end, the bulk modulus K_{s1} associated with the pressure p_{s1} in eqn (35i) is defined by the expression

$$K_{s1} = -J_s \frac{\hat{c} p_{s1}}{\hat{c} J_s}\bigg|_{\eta_{s1}}, \tag{92}$$

where the derivative is taken holding the entropy η_{s1} constant. Now, with the help of the expressions (35b,i) it may be shown that

$$K_{s1} = \rho_{s0} J_s \left[\frac{\mathrm{d}^2 \varepsilon_{s0}}{\mathrm{d}J_s^2} + \frac{C_s}{2} \frac{\mathrm{d}^2 \theta_s}{\mathrm{d}J_s^2} \coth\left\{\frac{\theta_s}{2\theta}\right\} \right]. \tag{93}$$

Next, eqn (35k) is used to identify the term $J_s^{-1}\hat{\mu}_s$ as the effective shear modulus. Then, the effective shear modulus is assumed to be related to the bulk modulus K_{s1} and the constant Poisson's ratio ν by the expression

$$J_s^{-1}\hat{\mu}_s = \frac{3(1-2\nu)}{2(1+\nu)} K_{s1}. \tag{94}$$

Similarly, eqns (43a,d) may be used to express the bulk modulus K_f of the fluid in compression $[J_f < F_f(\theta)]$ in a form similar to eqn (93)

$$K_f = -J_f \frac{\hat{c} p_f}{\hat{c} J_f}\bigg|_{\eta_f} = \rho_{f0} J_f \left[\frac{\mathrm{d}^2 \varepsilon_{f0}}{\mathrm{d}J_f^2} + \frac{C_f}{2} \frac{\mathrm{d}^2 \theta_f}{\mathrm{d}J_f^2} \coth\left\{\frac{\theta_f}{2\theta}\right\} \right]. \tag{95}$$

Since computer codes which predict the dynamic response of materials require an estimate of the sound speed in the material to control the time step size, it is desirable to develop an estimate of the bulk modulus. To this end, the simplified expression (73) for compressed constituents ($\hat{\phi} = \phi_1$, $\hat{J}_f = J_f$) is used together with a definition of the bulk modulus K to deduce that

$$K = -J \frac{\hat{c} p}{\hat{c} J} = \left[1 - \frac{J}{1-\phi} \frac{\hat{c}\phi}{\hat{c} J}\right]^2 (1-\phi) K_s + \left[1 + \frac{J}{\phi} \frac{\hat{c}\phi}{\hat{c} J}\right]^2 \phi K_f + (p_s - p_f)\left[2J \frac{\partial \phi}{\partial J} + J^2 \frac{\partial^2 \phi}{\partial J^2}\right]. \tag{96}$$

In developing the expression (96), derivatives of p_s and p_f with respect to J_s and J_f, respectively, were approximated by the formulas (92) and (95), even though the entropies η_{s1} and η_f cannot both be held constant simultaneously. Next, it is noted that in the absence

of fluid pressure the unloaded state ($J_s = 1$, $\beta = 1$) at reference temperature θ_0 yields the expression

$$K_0 = (1-\phi_0)(1-a)^2 K_{s0} \tag{97}$$

for the unloaded value K_0 of the bulk modulus in terms of the unloaded value K_{s0} of the bulk modulus of the solid. This expression shows that the value of a can be determined by the value of K_0 of the dry porous material.

At this point it is worth emphasizing that since the constitutive equations developed here are hyperelastic, the pressure p_s and p_f are determined by eqns (35h) and (43d). This is in contrast with a hypoelastic constitutive equation which integrates an expression for the rate of change of pressure using a specified form of the bulk modulus.

5. DETERMINATION OF CONSTITUTIVE FUNCTIONS FOR MT. HELEN TUFF

In this section, attention is focused on determining a consistent set of material constants and functions which model the response of Mt. Helen tuff to hydrostatic isothermal loading for dry and partially saturated conditions as determined by the experiments of Heard *et al.* (1973).

The constitutive equations of Section 4 require characterization of the response of the porous solid matrix by the material constants and functions

$$\{\rho_{s0}, C_s, \theta_{s0}, \nu\}, \quad \{p_{sH}(J_s), \varepsilon_{sH}(J_s), \gamma_s(J_s)\}, \tag{98a,b}$$

$$\{a, b\}, \quad \{b_s, F_s(\theta)\}, \tag{98c,d}$$

$$\{\Phi, \theta_0\}, \quad \{f(\phi), h_M, \theta_{Ms}(J_s), n, \kappa_d\}, \tag{98e,f}$$

$$\{g(U), K\}, \tag{98g}$$

and characterization of the fluid by the material constants and functions

$$\{\rho_{f0}, C_f, \theta_{f0}\}, \quad \{p_{fH}(J_f), \varepsilon_{fH}(J_f), \gamma_f(J_f)\}, \tag{99a,b}$$

$$\{S\}, \quad \{b_f, F_f(\theta)\}. \tag{99c,d}$$

and specification of the initial values of $\{\mathbf{B}_e', \kappa, \phi_u\}$ used to integrate the evolution equations (22) and (28a,b). The reference density ρ_0 of the mixture is determined by the expression (58). Also, for all calculations in this section, $\mathbf{B}_e'$ is set equal to $\mathbf{I}$.

If strength effects are ignored in the solid and the Hugoniot data are obtained from shock experiments on material which is initially in a stress-free reference state, then the internal energies ε_{sH} and ε_{fH} are related to the pressures p_{sH} and p_{fH} by the formulas

$$\rho_{s0}\varepsilon_{sH}(J_s) = \tfrac{1}{2}p_{sH}(J_s)(1-J_s), \tag{100a}$$

$$\rho_{f0}\varepsilon_{fH}(J_f) = \tfrac{1}{2}p_{fH}(J_f)(1-J_f). \tag{100b}$$

Moreover, the Hugoniot pressures p_{sH} and p_{fH} can be related to the shock velocities D_s and D_f and particle velocities u_s and u_f, of the solid and fluid, respectively, by the formulas

$$p_{sH} = \rho_{s0} D_s u_s, \quad p_{fH} = \rho_{f0} D_f u_f, \tag{101a,b}$$

with the relative volumes J_s and J_f given by

Table 1. Initial mass density ρ_0; comparison of computed values using eqns (57) and (103) with measurements of Heard *et al.* (1973)

Saturation S	Theoretical ρ_0 (Mg m^{-3})	Experimental ρ_0 (Mg m^{-3})
0	1.44	1.48
0.69	1.70	1.64
0.995	1.82	1.86

$$J_s = 1 - \frac{u_s}{D_s}, \quad J_f = 1 - \frac{u_f}{D_f}. \tag{102a,b}$$

Heard *et al.* (1973) measured the average grain density ρ_{s0} and the reference porosity Φ in the range 0.35–0.39 for Mt. Helen tuff so that ρ_{s0}, Φ and ρ_{f0} are specified by

$$\rho_{s0} = 2.32\,\text{Mg m}^{-3}, \quad \Phi = 0.38, \quad \rho_{f0} = 1\,\text{Mg m}^{-3}. \tag{103a,b,c}$$

Table 1 compares the values of ρ_0 calculated using the specification (103) and the formula (57) with the measured experimental values of ρ_0 for dry ($S = 0$), partially saturated ($S = 0.69$) and near fully saturated ($S = 0.995$) material. Given the measured range of initial porosity, these theoretical values of ρ_0 are considered to be reasonable.

Although this tuff is not a pure material, it is assumed that the functional forms for $D_s(u_s)$ and $\gamma_s(J_s)$ can be related to those given for silicon dioxide by multiplying by an appropriate function of the ratio of the reference densities. Using the equation of state reported by Ree (1976a) and noting that the reference density of silicon dioxide is 2.65 Mg m^{-3}, the functional forms for D_s and γ_s characterizing tuff are specified by

$$D_s(u_s) = \left(\frac{2.65}{2.32}\right)^{1/2}[3.69] \qquad \text{for} \quad u_s < 0, \tag{104a}$$

$$D_s(u_s) = \left(\frac{2.65}{2.32}\right)^{1/2}[3.69 + 1.85u_s - 0.6374u_s^2 + 0.16695u_s^3 - 1.1893\times 10^{-2}u_s^4 - 9.0375\times 10^{-5}u_s^5], \qquad \text{for} \quad u_s \geqslant 0, \tag{104b}$$

$$\gamma_s(J_s) = 0.5 + \left[\gamma_s\left(\frac{1}{2}\right) - 0.5\right](2J_s) \quad \text{for} \quad J_s < \frac{1}{2}, \tag{104c}$$

$$\gamma_s(J_s) = \left(\frac{2.65}{2.32}\right)\left[0.6 + \left\{\frac{1}{J_s} - 1\right\}^3\right] \quad \text{for} \quad \frac{1}{2} \leqslant J_s \leqslant 1, \tag{104d}$$

$$\gamma_s(J_s) = \gamma_s(1) \approx 0.5253 \qquad \text{for} \quad J_s > 1, \tag{104e}$$

where D_s and u_s are measured in km s^{-1}. In eqns (104), D_s and γ_s are scaled so that the reference values of the bulk modulus and $\rho_{s0}\gamma_s$ for tuff are equal to those for silicon dioxide. The extension (104c) for high compression was suggested by Young (1994).

Similarly, using the equation of state of water reported by Ree (1976b), the functional forms for $D_f(u_f)$ and $\gamma_f(J_f)$ are specified by

$$D_f(u_f) = 1.4829 \quad \text{for} \quad u_f < 0, \tag{105a}$$

$$D_f(u_f) = 1.4829 + 2.1057u_f - 0.1744u_f^2 + 0.010085u_f^3 \quad \text{for} \quad u_f \geqslant 0, \tag{105b}$$

$$\gamma_f(J_f) = 0.5 + [\gamma_f(0.45) - 0.5]\left(\frac{J_s}{0.45}\right) \quad \text{for} \quad J_f < 0.45, \tag{105c}$$

$$\gamma_f(J_f) = -239.703 + 3081.87V - 16345.9V^2 + 46506.6V^3 - 76706.8V^4 + 73499.3V^5 - 37987.4V^6 + 8192.56V^7 \quad \text{for} \quad 0.45 \leqslant J_f \leqslant 1, \tag{105d}$$

$$V = 1.0018J_s, \tag{105e}$$

$$\gamma_f(J_f) = \gamma_f(1) \approx 0.5348, \quad \text{for} \quad J_f > 1, \tag{105f}$$

where again D_f and u_f are measured in km s^{-1} and the extension (105c) for high compression was suggested by Young (1994).

The reference temperature is specified by

$$\theta_0 = 300\,\text{K}. \tag{106}$$

and the values of $\{C_s, \theta_{s0}, C_f, \theta_{f0}\}$ were suggested by Young (1994) to be

$$C_s = 1247\,\text{J kg}^{-1}\,\text{K}^{-1}, \quad \theta_{s0} = 1000\,\text{K}, \tag{107a, b}$$

$$C_f = 4157\,\text{J kg}^{-1}\,\text{K}^{-1}, \quad \theta_{f0} = 100\,\text{K}. \tag{107c, d}$$

Using these specifications together with linear interpolations of the functions $\{D_s(u_s), \gamma_s(J_s), D_f(u_f), \gamma_f(J_f)\}$, eqns (39) and (47) were integrated numerically subject to the reference conditions (36a), (40), and (44a), (48) to generate tables of the functions $\theta_s(J_s)$, $\varepsilon_{s0}(J_s)$, $\theta_f(J_f)$ and $\varepsilon_{f0}(J_f)$, and of their derivatives up to order three, which are needed to determine derivatives of the shear modulus $\hat{\mu}_s$ in eqn (94). Also, the expressions (35i) and (43d) were used to solve eqns (51) and (59) for temperature to generate additional tables of $F_s(\theta)$ and $F_f(\theta)$ and their first derivatives. In this regard, it is noted that eqns (51) and (59) have no real solutions for temperature when the relative volume becomes smaller than certain critical values. This indicates that it is impossible to cool the material sufficiently to cause the pressure to vanish at high levels of compression.

The values of b_s and b_f are specified arbitrarily by

$$b_s = 10^{-4}, \quad b_f = 10^{-4}. \tag{108a, b}$$

but they could be determined by attempting to match maximum tensile values for p_{s1} and p_f. To check the computer coding of the constitutive equations, loading along the Hugoniot (from $J = 1$) and unloading along an adiabat or an isotherm (to $J > 1$) were simulated for both the solid and fluid, and the results for pressure and temperature are shown in Fig. 1. To calculate the loading along the Hugoniot the internal energy was specified by one of the formulas (100a,b). Since the thermal effect in the solid is relatively small the adiabat and isotherm are close to one another so the adiabat is not shown in Fig. 1(a–c). For the solid, the value of a in eqn (61a) was set equal to zero so that $\phi_1 = \phi_u$. Also, the values of ϕ_u and Φ were specified by 10^{-5} to simulate the response of a nearly nonporous solid. Notice from

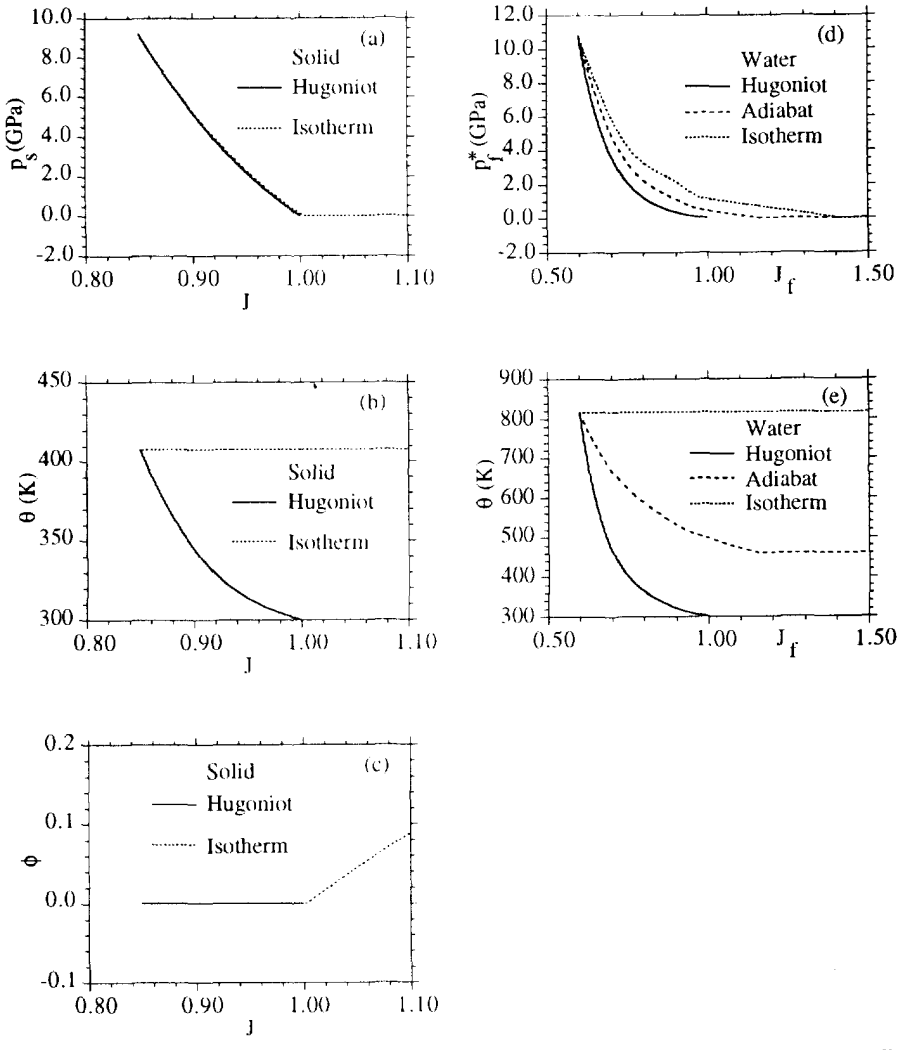

Fig. 1. Shock loading Hugoniot curves with adiabatic or isothermal unloading for nonporous tuff (a–c) and water (d, e).

Fig. 1(a) and (c) that the analytical extension of the constitutive equation for the solid into the expansion region causes the pressure in the solid to remain near zero and the porosity ϕ to increase rapidly as J expands greater than the value $F_s(\theta)$ associated with zero pressure. This simulates increased porosity due to failure in tension. The results for water shown in Fig. 1(d) and (e) show more clearly that the formulation causes the pressure to remain near zero at the appropriate values of J_f [$J_f \geq F_f(\theta)$]. The relatively complicated structure of the isotherm of water shown in Fig. 1(d) for $J_f < 1$ is due to the complicated form of $\gamma_f(J_f)$ given by eqn (105d). As a further test of the computer simulation, the Hugoniot curves shown in Fig. 1(a,d), which were calculated using the constitutive equations of Section 4, were compared with the analytical forms (101) and shown to be identical. This indicates that the integration of eqns (39) and (47) is quite accurate.

Figure 2 shows the experimental data for dry ($S = 0$) Mt. Helen tuff measured by Heard *et al.* (1973) for isothermal hydrostatic loading and unloading from various pressures. Here, the unloading curve from 3.9 GPa is assumed to be elastic and is used to determine the values for the constants a and b in eqn (61a), which are given by

$$a = 0.657, \quad b = 1.15. \tag{109a,b}$$

Specifically, since the material is dry and at reference temperature θ_0, the unloaded value of J_s is $J_s = 1$, so that $\phi_u = 0.240$ for this unloading curve. Using this constant value of ϕ_u

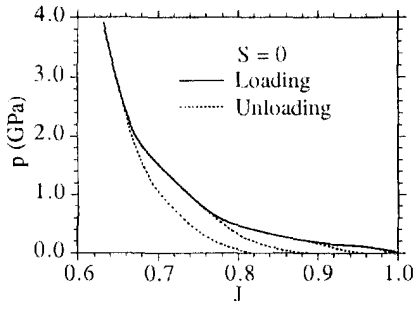

Fig. 2. Experimental loading and unloading curves for dry ($S = 0$) Mt. Helen tuff reported by Heard *et al.* (1973)

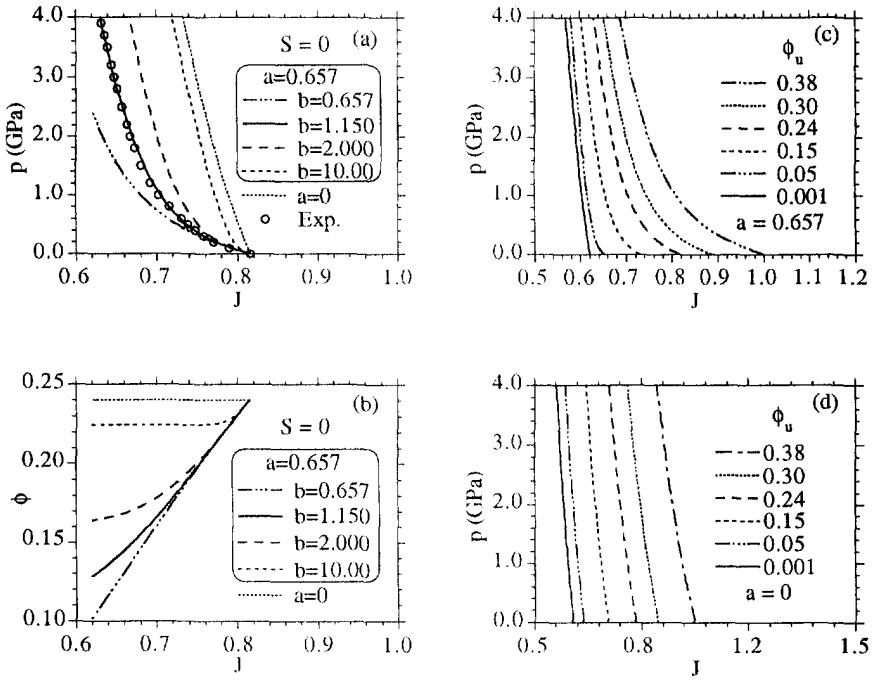

Fig. 3. Influence of the parameter b for soft response with $a = 0.657$; comparison with stiff response ($a = 0$) and comparison with unloading experimental data. Also, influence of changing ϕ_u on elastic loading curves for soft and stiff responses.

the elastic compression curve can be calculated for different values of a and b. Figure 3(a,b) shows the isothermal response for a given by eqn (109a) and various values of b, as well as the result for $a = 0$, which causes loading at constant porosity ($\phi = \phi_u$). The value of a determines the slope of the unloading curve at zero pressure and the value of b controls its shape. Moreover, the curve for $a = 0$ which causes compression at constant porosity shows that the added compressibility of porosity ($a > 0$) is needed to match the experimental data. For convenience, the material associated with the specification (109) will be referred to as the soft material and the material associated with the specification $a = 0$ will be referred to as the stiff material. Figure 3(c,d) shows isothermal compression for various constant values of unloaded porosity ϕ_u. In particular, notice that shape of the compression curve for the soft material [Fig. 3(c)] change significantly as the material is compacted and ϕ_u decreases, whereas the shape for the stiff material [Fig. 3(d)] is much less affected by changes in ϕ_u.

Another indication of the need for this added compressibility of porosity is shown in Fig. 4, which compares the initial elastic loading curves for the soft and stiff materials (each with $\phi_u = \Phi$) with the experimental compaction curve. This figure indicates that the elastic wave speed associated with the soft material will be reasonable and that the initial wave

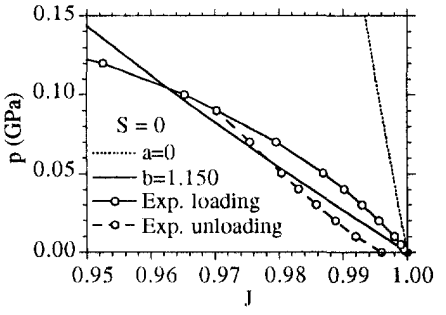

Fig. 4. Comparison of stiff ($a = 0$) and soft ($b = 1.150$) material response at constant porosity with loading and unloading experimental data.

speed for the stiff material will be much too fast. Also, the experimental data shown in Fig. 4 indicate that the initial portion of the compaction curve (loading) may not be representative of the elastic response of the partially crushed material, because the unloading curve exhibits a substantially softer response.

In the remaining simulations the initial value of ϕ_u is taken to be

$$\phi_u = \Phi \quad \text{for} \quad t = 0. \tag{110}$$

Instead of determining Γ_ϕ by the consistency conditions discussed in Appendix A and integrating the evolution eqn (28b), the value of ϕ_u is determined by satisfying the compaction and dilation constraints $g_c \leqslant 0$ and $g_d \leqslant 0$ directly. More specifically, trial values g_c^* and g_d^* of the compaction and dilation surfaces g_c and g_d are determined by assuming that ϕ_u remains constant. If g_c^* and g_d^* are both nonpositive then ϕ_u is unchanged. If g_c^* is positive then compaction must occur and ϕ_u is decreased iteratively until $g_c = 0$. On the other hand, if g_d^* is positive then dilation must occur and ϕ_u is increased until $g_d = 0$.

Also, in the remaining simulations the value of κ_d is arbitrarily specified to be

$$\kappa_d = 10.0\,\text{MPa}, \tag{111}$$

which keeps the magnitude of effective pressure p_c relatively low during dilation. Moreover, for the isothermal simulations considered next it is not necessary to specify values for h_M and n characterizing the function h in eqn (90b), since $h = 1$ for $\theta = \theta_0$.

Once the material constants characterizing the thermoelastic response are specified, the value of $f(\phi)$ in the compaction surface (88a) can be determined by matching the experimental isothermal ($\theta = \theta_0$; $h = 1$) loading curve for the dry material. This is done by iteratively solving for the value of ϕ_u which causes g_c to vanish for each of the experimental points. Thus, the isothermal loading curve of the theory exactly reproduces the experimental loading curve once compaction occurs ($g_c = 0$). The isothermal response to cycles of loading, unloading and reloading for the soft and stiff materials are shown in Fig. 5. Figure 5(a) shows that the soft response matches the experimental data quite well for unloading from pressures lower than 3.9 GPa, even though the material parameters (109) were determined by matching only the unloading curve from this high pressure. Figure 5(b) shows that the elastic unloading of the stiff material, which occurs at constant porosity, does not capture the correct unloading response at any pressure, even though the loading curve is correct. In this regard, it should be mentioned that the analysis of Bhatt *et al.* (1975) suggests that pore recovery during unloading from 3.9 GPa is a dissipational process. In contrast, here this pore recovery is modeled as a reversible elastic process because unloading and reloading occur on the same curves until the compaction or dilation constraints are activated.

Figure 5(c) shows the calculated forms of the compaction function $f(\phi)$ for both the soft and stiff materials. In order to extend the applicability of the theory beyond the range

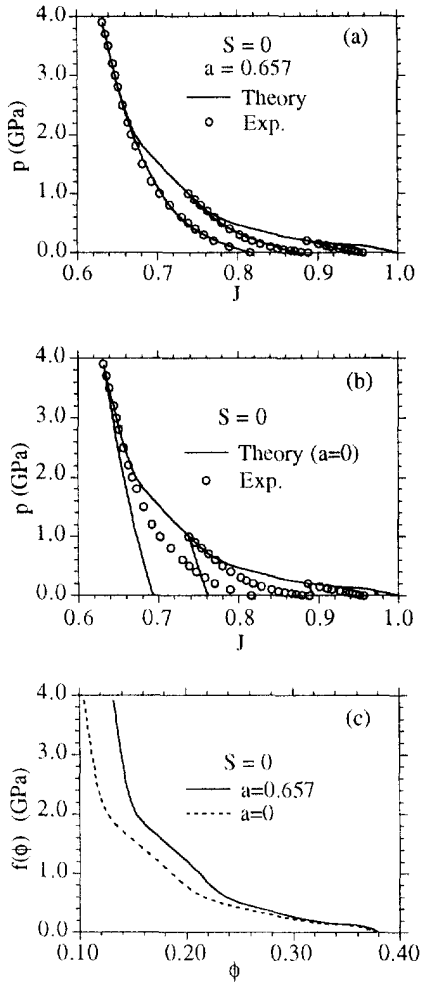

Fig. 5. Comparison of soft ($a = 0.657$) and stiff ($a = 0$) dry ($S = 0$) material response with loading and unloading experimental data.

($\phi_{\min} \leqslant \phi \leqslant \Phi$) determined by the experimental data, analytical extensions for $f(\phi)$ are specified by

$$f(\phi) = \frac{A}{\phi^m} \quad \text{for} \quad \phi \leqslant \phi_{\min}, \tag{112a}$$

$$f(\phi) = 0 \quad \text{for} \quad \phi \geqslant \Phi, \tag{112b}$$

where $\phi_{\min}$ is the minimum value of ϕ determined by the experimental loading curve. The values of the constants A and m are determined by demanding continuity of f and $\mathrm{d}f/\mathrm{d}\phi$ at $\phi = \phi_{\min}$, so that

$$m = -\frac{\phi_{\min}\dfrac{\mathrm{d}f}{\mathrm{d}\phi}(\phi_{\min})}{f(\phi_{\min})}, \quad A = (\phi_{\min})^m f(\phi_{\min}). \tag{113a,b}$$

For the soft material A, m and $\phi_{\min}$ are specified by

$$A = 0.872\,\text{MPa}, \quad m = 4.16, \quad \phi_{\min} = 0.132, \tag{114a,b}$$

and for the stiff material A, m and $\phi_{\min}$ are specified by

$$A = 1.03\,\text{MPa}, \quad m = 3.66, \quad \phi_{\min} = 0.105. \tag{115a,b}$$

The functional form (112a) includes a singularity as ϕ approaches zero, which is necessary for satisfaction of the compaction constraint as the pressure increases and the material response is dominated by that of the nonporous solid. In addition, for numerical purposes it may be desirable to ignore small changes in porosity as ϕ approaches zero by setting $f = \infty$ when ϕ decreases below some critical value. Also, if detailed experimental data are not available, then it is possible to specify $f(\phi)$ in terms of a few material constants using one of the analytical forms that have been developed (e.g. Bhatt *et al.*, 1975; Butkovich, 1973; Carroll and Kim, 1984; Oh and Persson, 1989; Wang, 1994).

At this point, all the material parameters characterizing isothermal response have been specified, so that the following simulations of nearly saturated response and partially saturated response test the predictive capability of the theory. Figure 6 shows a comparison of theoretical predictions with experimental data for isothermal compaction of nearly saturated ($S = 0.995$) material. Figure 6(a–d) shows the response of the soft material and Fig. 6(e–g) the response of the stiff material. The experimental data in Fig. 6(a,e) exhibit the results of two known phase transformations of water: one from liquid to ice VI at about 1.0 GPa and one from ice VI to ice VII at about 2.2 GPa (Reser, 1979, p. 525). These phase transformations of water are not modeled by the constitutive equation which is based on the shock data (105).

The theoretical predictions of the soft material [Fig. 6(a)] and the stiff material [Fig. 6(e)] both indicate good agreement with the experimental data. In order to better understand this response, additional simulations were performed which: (a) eliminated the compaction constraint by setting $f = \infty$, and (b) caused pressure equilibrium between the solid and the fluid ($p_e = 0$) by setting $f = 0$. The simulations in Fig. 6 denoted by Theory used the functional forms for $f(\phi)$ shown in Fig. 5(c), which were determined by the experimental dry loading curve.

For the soft material the effective pressure [Fig. 6(b)] remains low enough that the constraint due to the compaction surface is never activated, so the responses predicted by the Theory and $f = \infty$ in Fig. 6(a–d) are identical. This indicates that the model (61a) for the added compressibility of porosity which causes ϕ to decrease during compression at constant ϕ_u predicts reasonable response for the nearly saturated case, even though it was determined from dry data. This conclusion is further supported by the fact that the stiff material with $f = \infty$ shown in Fig. 6(e) predicts much too stiff a response, since porosity remains constant during the compression [see Fig. 6(g)]. In this regard, it is also noted from Fig. 6(b) that as compression increases the effective pressure increases to a maximum and then decreases to a negative value, at which time the dilation constraint is activated. This indicates that the model (61a) for the added compressibility of porosity does not accurately predict details of the material response at high pressure because the effective pressure is expected to remain positive in this situation. However, the overall response predicted by the model remains reasonable because the dilation surface keeps the effective pressure from becoming too negative. Moreover, even though the dilation surface is activated [when ϕ_u increases in Fig. 6(d)] the porosity ϕ in Fig. 6(c) continues to decrease.

The responses of both the soft and stiff materials for $f = 0$ also match the experimental data quite well. This indicates that to first order the compression of a composite of tuff and water can be modeled by demanding pressure equilibrium between the tuff and water constituents. Consequently, the local effects of deviatoric stress near pores in the solid matrix which cause significant effective pressure in the dry material seem to be negligible in the saturated material.

Figure 7 shows the predicted response for partially saturated soft material. The value $S = 0.69$ was determined by matching the point at which the pores collapse sufficiently to

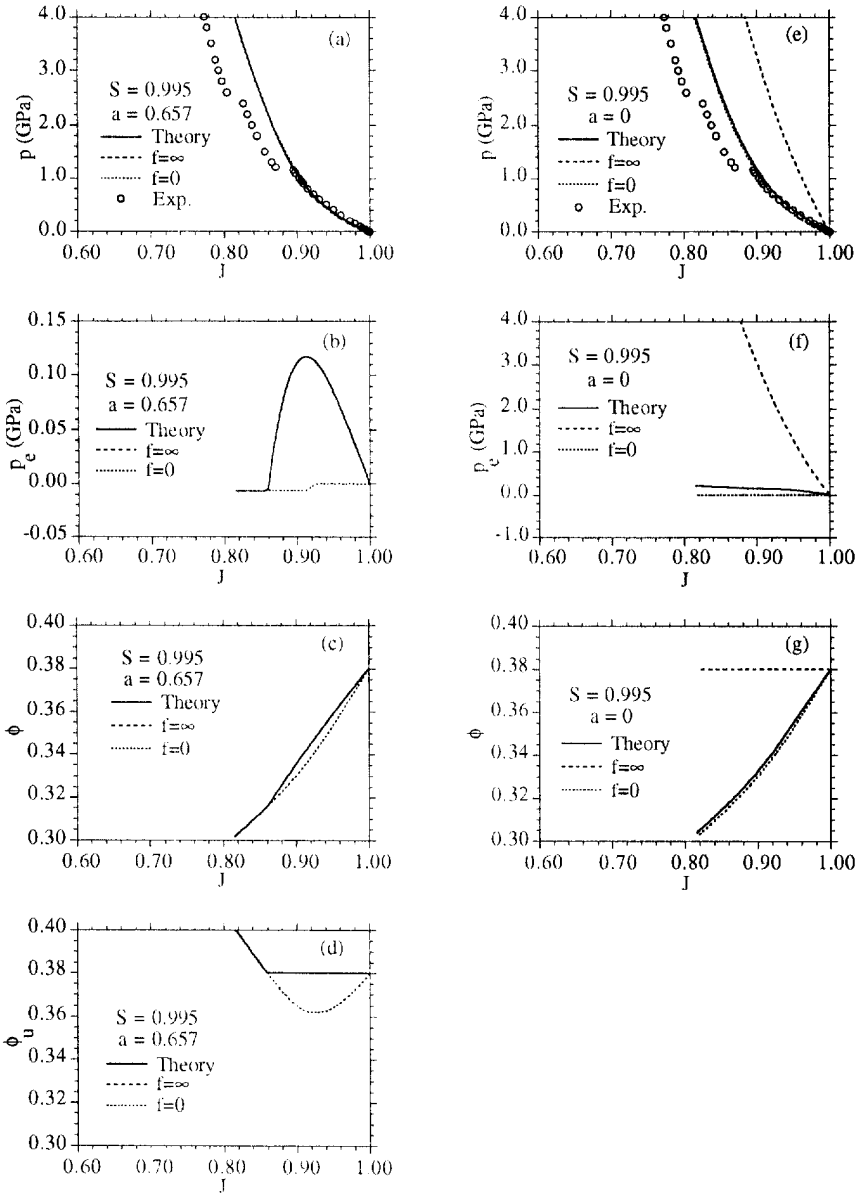

Fig. 6. Comparison of theory and experiment for nearly saturated response with $S = 0.995$.

become saturated. At this point the fluid pressure and total pressure both begin to increase rapidly.

The remaining simulations show predictions of the Hugoniot curves for dry ($S = 0$), partially saturated ($S = 0.69$) and nearly saturated ($S = 0.995$) soft material. For determining the Hugoniot curves the internal energy ε is related to the density ρ_0 [see eqn (57) and Table 1] and the pressure p by the expression

$$\rho_0 \varepsilon = \tfrac{1}{2} p(1 - J), \tag{116}$$

which is used to determine the value of temperature. Since temperature increases along the Hugoniot, it is necessary to specify values for the constants determining the function h in the compaction and dilation surfaces (88) and (89). For the present purposes h_M, n, and $\theta_{Ms}(J_s)$ are taken to be

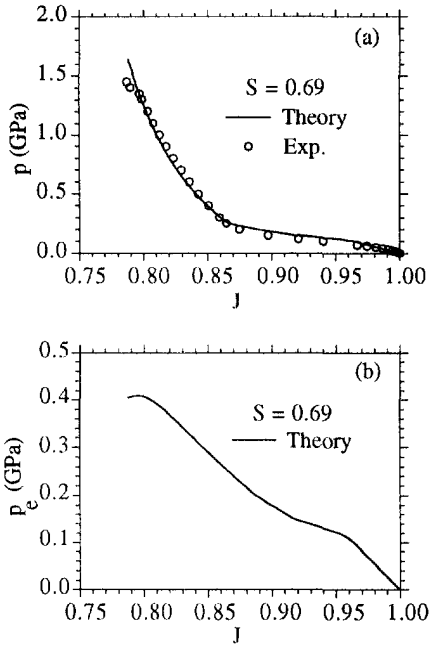

Fig. 7. Comparison of theory and experiment for partially saturated response with $S = 0.69$.

$$h_M = 10^{-6}, \quad n = 0.1, \quad \theta_{M_s}(J_s) = 2000\,\text{K}. \tag{117a,b,c}$$

The constant value of θ_{M_s} is a reasonable estimate of the melting temperature of silicon dioxide (Young, 1994). Although no experimental data were used to determine h_M and n, the values (117a, b) will cause a rapid drop in the function h when the solid melts ($\theta = \theta_{M_s}$).

To evaluate the influence of melting on the compaction surface, the Hugoniot of the dry material was calculated using the specifications (117) as well as using the specification $n = 0$, which eliminates thermal dependence of h (since $h = 1$). Figure 8 shows that when the solid melts ($\theta = 2$ kK), the pressure and temperature on the Hugoniot drop rapidly as the porosity decreases to a value near zero. As compression continues, the porosity ϕ continues to decrease and the magnitude of the pressure is controlled by the pressure response of the nonporous solid, since $f(\phi)$ is singular at $\phi = 0$. This predicted response is physically reasonable because at melting the solid can no longer support nonzero deviatoric stresses concentrated around open pores.

Figure 9 shows the Hugoniot curves for the specification (117). Also shown in Fig. 9(e) are curves of shock velocity D vs particle velocity u determined by the formulas

$$D = \left[\frac{p}{\rho_0(1-J)}\right]^{1/2}, \quad u = D(1-J). \tag{118a,b}$$

Notice that for both the partially and nearly saturated cases, the effective pressure p_e remains small. Also, notice that the porosity continues to decrease even when the effective pressure becomes slightly negative and the dilation surface is activated.

6. SUMMARY

Constitutive equations have been developed to describe the thermomechanical response of a porous brittle solid whose pores may be dry or partially filled with fluid. For simplicity and the specific application of interest, the solid and fluid are assumed to have no relative motion and are assumed to have the same temperature. This means that constitutive equations for the composite of porous solid and fluid can be developed within the context of the thermomechanical theory of a simple continuum. A functional form for the Helmholtz

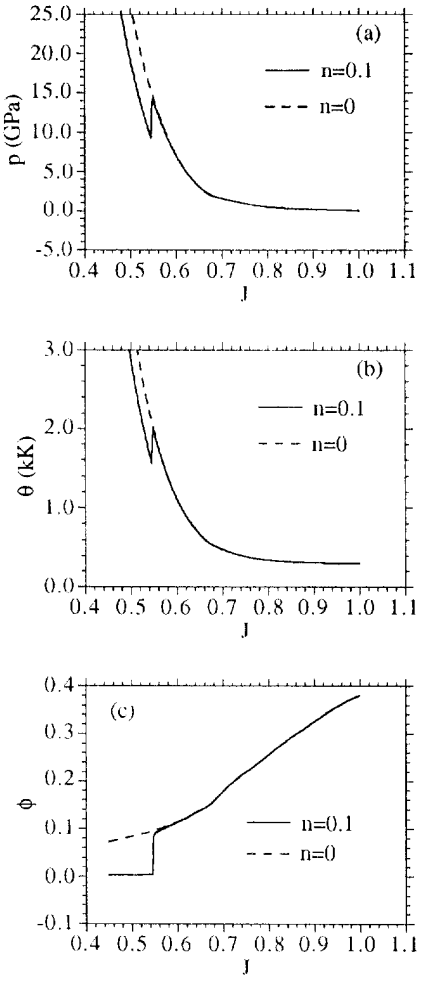

Fig. 8. Hugoniot curves predicted for dry material showing the influence of pore collapse due to melting ($n = 0.1$).

free energy of the composite is proposed in terms of known Helmholtz free energies of the nonporous solid and the fluid, and restrictions on the constitutive assumptions due to the first and second laws of thermodynamics are satisfied. Also, the porosity is used to model added compressibility observed in porous dry materials as well as to describe features of the interaction of the fluid with the surrounding solid matrix. Although the constitutive equations model distortional plasticity, which limits the magnitude of the deviatoric stress, attention has been mainly focused on the development of specific equations for predicting the response to hydrostatic external pressure.

Since the model attempts to predict physically reasonable response over a wide range of pressure and temperature, it is necessary to provide a theoretical structure that can accommodate known high pressure equations of state deduced from shock experiments. In this regard, it is mentioned that the Helmholtz free energies of the solid and fluid constituents use an Einstein formulation with variable specific heat, and are consistent with Mie–Grüneisen equations (for part of the pressure) which accommodate general expressions for shock velocity as a function of particle velocity and Grüneisen gamma as a function of relative density.

Although the function $f(\phi)$ which characterizes compaction is determined by matching dry compaction data, the predictions of the model compare well with experimental data for pressure measured during isothermal compression of both partially saturated and near fully saturated material. Furthermore, these simulations indicate that accurate prediction of effective pressure p_e is quite difficult in the high pressure regime because p_e is the difference

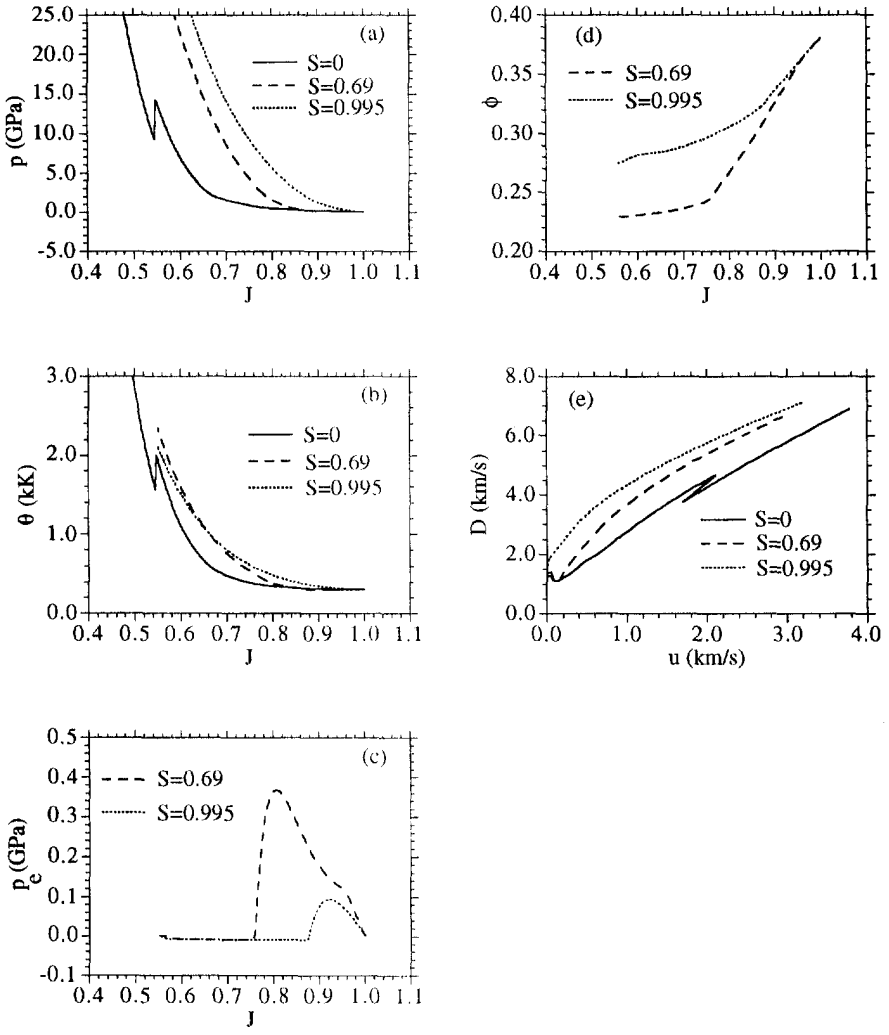

Fig. 9. Hugoniot curves predicted for dry ($S = 0$), partially saturated ($S = 0.69$) and nearly saturated ($S = 0.995$) material with $n = 0.1$.

between two large pressures p and $p_f^*$and because the predicted value of p_e is quite sensitive to the specific theoretical model for reversible porosity changes. This suggests that the Terzaghi assumption that yield strength $Y(p_e)$ is a function of p_e only will probably not be very accurate in the high pressure regime, since p_e cannot be predicted accurately there. Consequently, it may be more desirable to use $Y(p_e)$ when the total pressure p remains relatively small and then use a more complicated function of p and p_e when p becomes large. Also, it is important to understand the influence of damage evolution as the material compacts and grains are presumably fractured.

Using a different model from that presented here, Attia and Rubin (1993) examined the influence of soft and stiff unloading on spherically symmetric wave propagation. Their results indicate that soft unloading [similar to that shown in Fig. 5(a)] creates a slower release wave relative to stiff unloading [similar to that shown in Fig. 5(b)]. This slower release wave causes the radial velocity time history at a given radial position to exhibit a significantly greater peak velocity than that associated with the stiff unloading. Furthermore, preliminary spherically symmetric wave propagation calculations using the present model indicate that different functional forms of the yield strength $Y(p, p_e)$ can significantly change velocity profiles. However, substantial additional study is needed to determine what functional forms may be most physically reasonable.

Acknowledgements—The authors would like to acknowledge helpful discussions with Drs L. Glenn and D. Young. Part of this work was performed under the auspices of the United States Department of Energy at Lawrence

Livermore National Laboratory under Contract No. W-7405-ENG-48 while M. B. Rubin was on leave from Technion, and part was supported specifically by the Geosciences Research Program of the Department of Energy Office of Energy Research within the Office of Basic Energy Sciences, Division of Engineering and Geosciences.

REFERENCES

Attia, A. V. and Rubin, M. B. (1993). The effect of dilatancy on the unloading behavior of Mt. Helen tuff. In *Proc. Numerical Modeling For Underground Nuclear Test Monitoring Symp.*, Durango, CO, 23–25 March 1993. Los Alamos National Laboratory Report No. LA-UR-93-3839.

Baer, M. R. (1988). Numerical studies of dynamic compaction of inert and energetic granular materials. *ASME J. Appl. Mech.* **55,** 36–43.

Baer, M. R. and Nunziato, J. W. (1986). A two-phase mixture theory for the deflagration-to-detonation transition (DDT) in reactive granular materials. *Int. J. Multiphase Flow* **12,** 861–889.

Besseling, J. F. (1966). A thermodynamic approach to rheology. *Proc. IUTAM Symp. on Irreversible Aspects of Continuum Mechanics and Transfer of Physical Characteristics in Moving Fluids*, Vienna (Edited by H. Parkus and L. I. Sedov), pp. 16–53. Springer, Vienna.

Bhatt, J. J., Carroll, M. M. and Schatz, J. F. (1975). A spherical model calculation for volumetric response of porous rocks. *ASME J. Appl. Mech.* **42,** 363–368.

Butkovich, T. R. (1973). A technique for generating pressure–volume relations and failure envelopes for rocks. Report No. UCRL-51441, Lawrence Livermore National Laboratory, Livermore, CA.

Carroll, M. M. (1980). Mechanical response of fluid-saturated porous materials. In *Theoretical and Applied Mechanics* (Edited by F. P. J. Rimrott and B. Tabarrok), pp. 251–262. North-Holland, Amsterdam.

Carroll, M. M. and Holt, A. C. (1972a). Suggested modification of the P–α model for porous materials. *J. Appl. Phys.* **43,** 759–761.

Carroll, M. M. and Holt, A. C. (1972b). Static and dynamic pore-collapse relations for ductile porous materials. *J. Appl. Phys.* **43,** 1626–1635.

Carroll, M. M. and Kim, K. T. (1984). Pressure–density equations for porous metals and metal powders. *Powder Metall.* **27,** 153–159.

DiMaggio, F. L. and Sandler, I. S. (1971). Material model for granular soil. *ASCE J. Engng Mech.* **97,** 935–950.

Drumheller, D. S. (1987a). Hypervelocity impact of mixtures. *Int. J. Impact Engng* **5,** 261–268.

Drumheller, D. S. (1987b). A theory for dynamic compaction of wet porous solids. *Int. J. Solids Structures* **23,** 211–237.

Drumheller, D. S. and Bedford, A. (1980). A thermomechanical theory for reacting immiscible mixtures. *Arch. Rational Mech. Anal.* **73,** 257–284.

Eckart, C. (1948). The thermodynamics of irreversible processes. IV. The theory of elasticity and anelasticity. *Phys. Rev.* **73,** 373–382.

Embid, P. and Baer, M. (1992). Mathematical analysis of a two-phase continuum mixture theory. *Continuum Mech. Thermodyn.* **4,** 279–312.

Eringen, A. C. (1994). A continuum theory of swelling porous elastic soils. *Int. J. Engng Sci.* **32,** 1337–1349.

Flory, P. (1961). Thermodynamic relations for high elastic materials. *Trans. Faraday Soc.* **57,** 829–838.

Goodman, M. A. and Cowin, S. C. (1972). A continuum theory for granular materials. *Arch. Rational Mech. Anal.* **44,** 249–266.

Green, A. E. and Naghdi, P. M. (1977). On thermodynamics and the nature of the second law. *Proc. R. Soc. Lond.* **A357,** 253–270.

Green, A. E. and Naghdi, P. M. (1978). The second law of thermodynamics and cyclic processes. *ASME J. Appl. Mech.* **45,** 487–492.

Gurson, A. L. (1977). Continuum theory of ductile rupture by void nucleation and growth: part I—Yield criteria and flow rules for porous ductile materials. *J. Engng Materials Tech.* **99,** 2–15.

Heard, H. C., Bonner, B. P., Duba, A. G., Shock, R. N. and Stephens, D. R. (1973). High pressure mechanical properties of Mt. Helen, Nevada, tuff. Report No. UCID-16261, Lawrence Livermore National Laboratory, Livermore, CA.

Herrmann, W. (1969). Constitutive equation for the dynamic compaction of ductile porous materials. *J. Appl. Phys.* **40,** 2490–2499.

Hill, T. L. (1960). *An Introduction To Statistical Thermodynamics*. Addison-Wesley, Reading, MA.

Jaeger, J. C. and Cook, N. G. W. (1976). *Fundamentals Of Rock Mechanics*. Halsted Press, New York.

Leonov, A. I. (1976). Nonequilibrium thermodynamics and rheology of viscoelastic polymer media. *Rheol. Acta* **15,** 85–98.

Li, X. (1994). Elastic coefficients for liquid- and gas-saturated porous media. *Int. J. Engng Sci.* **32,** 195–208.

Naghdi, P. M. and Trapp, J. A. (1975). The significance of formulating plasticity theory with reference to loading surfaces in strain space. *Int. J. Engng Sci.* **13,** 785–797.

Nunziato, J. W. and Walsh, E. K. (1980). On ideal mutiphase mixtures with chemical reactions and diffusion. *Arch. Rational Mech. Anal.* **73,** 285–311.

Oh, K.-H. and Persson, P.-A. (1989). A constitutive model for the shock Hugoniot of porous materials in the incomplete compaction regime. *J. Appl. Phys.* **66,** 4736–4742.

Ree, F. H. (1976a). Equation of state of the silicon dioxide system. No. UCRL-52153, Lawrence Livermore National Laboratory, Livermore, CA.

Ree, F. H. (1976b). Equation of state of water. No. UCRL-52190, Lawrence Livermore National Laboratory, Livermore, CA.

Reser, M. K. (1979). *Phase Diagrams for Ceramists*, 4th printing. The American Ceramic Society, Columbus, OH.

Rice, J. R. and Tracey, D. M. (1969). On the ductile enlargement of voids in triaxial stress fields. *J. Mech. Phys. Solids* **17,** 201–217.

Rubin, M. B. (1987). An elastic–viscoplastic model for metals subjected to high compression. *ASME J. Appl. Mech.* **54,** 532–538.
Rubin, M. B. (1989). A time integration procedure for plastic deformation in elastic–viscoplastic metals. *J. Appl. Math. Phys. (ZAMP)* **40,** 846–871.
Rubin, M. B. (1990). An elastic–viscoplastic model for large deformations of soils. *ASCE J. Engng Mech.* **116,** 1995–2015.
Rubin, M. B. (1992). Hyperbolic heat conduction and the second law. *Int. J. Engng Sci.* **30,** 1665–1676.
Rubin, M. B. (1994a). Plasticity theory formulated in terms of physically based microstructural variables—I. Theory. *Int. J. Solids Structures* **31,** 2615–2634.
Rubin, M. B. (1994b). Plasticity theory formulated in terms of physically based microstructural variables—II. Examples. *Int. J. Solids Structures* **31,** 2635–2652.
Rubin, M. B. and Attia, A. (1995). Calculation of hyperelastic response of finitely deformed elastic–viscoplastic materials. *Int. J. Numer. Meth. Engng.* In press.
Rubin, M. B. and Chen, R. (1991). Universal relations for elastically isotropic elastic–plastic materials. *ASME J. Appl. Mech.* **58,** 283–285.
Rubin, M. B. and Yarin, A. L. (1993). On the relationship between phenomenological models for elastic–viscoplastic metals and polymeric liquids. *J. Non-Newtonian Fluid Mech.* **50,** 79–88.
Wang, Z. P. (1994). Void growth and compaction relations for ductile porous materials under intense dynamic general loading conditions. *Int. J. Solids Structures* **31,** 2139–2150.
Young, D. A. (1994). Private communication. Lawrence Livermore National Laboratory.

APPENDIX A

In order to conveniently represent the various possible loading and unloading conditions associated with the surfaces g, g_c, g_d in eqn (27), it is desirable to first define the following functions:

$$\hat{g} = \left[J\frac{\partial g}{\partial J}\mathbf{I} + \frac{\partial g}{\partial \alpha_1}\{\mathbf{B}_e - \tfrac{1}{3}(\mathbf{B}_e\cdot\mathbf{I})\mathbf{I}\} + 2\frac{\partial g}{\partial \alpha_2}\{\mathbf{B}_e^2 - \tfrac{1}{3}(\mathbf{B}_e^2\cdot\mathbf{I})\mathbf{I}\}\right]\cdot\mathbf{D} + \frac{\partial g}{\partial\theta}\dot{\theta}, \tag{A1a}$$

$$\bar{g}_1 = -\left[\left\{\frac{\partial g}{\partial \alpha_1}\mathbf{I} + 2\frac{\partial g}{\partial \alpha_2}\mathbf{B}_e\right\}\cdot\tilde{\mathbf{A}} - \frac{\partial g}{\partial K}K\right], \quad \bar{g}_2 = -\left[\frac{\partial g}{\partial \phi_u}\right], \tag{A1b,c}$$

$$\hat{g}_c = \left[J\frac{\partial g_c}{\partial J}\mathbf{I} + \frac{\partial g_c}{\partial \alpha_1}\{\mathbf{B}_e - \tfrac{1}{3}(\mathbf{B}_e\cdot\mathbf{I})\mathbf{I}\} + 2\frac{\partial g_c}{\partial \alpha_2}\{\mathbf{B}_e^2 - \tfrac{1}{3}(\mathbf{B}_e^2\cdot\mathbf{I})\mathbf{I}\}\right]\cdot\mathbf{D} + \frac{\partial g_c}{\partial\theta}\dot{\theta}, \tag{A1d}$$

$$\bar{g}_{c1} = -\left[\left\{\frac{\partial g_c}{\partial \alpha_1}\mathbf{I} + 2\frac{\partial g_c}{\partial \alpha_2}\mathbf{B}_e\right\}\cdot\tilde{\mathbf{A}} + \frac{\partial g_c}{\partial K}K\right], \quad \bar{g}_{c2} = -\left[\frac{\partial g_c}{\partial \phi_u}\right], \tag{A1e,f}$$

$$\hat{g}_d = \left[J\frac{\partial g_d}{\partial J}\mathbf{I} + \frac{\partial g_d}{\partial \alpha_1}\{\mathbf{B}_e - \tfrac{1}{3}(\mathbf{B}_e\cdot\mathbf{I})\mathbf{I}\} + 2\frac{\partial g_d}{\partial \alpha_2}\{\mathbf{B}_e^2 - \tfrac{1}{3}(\mathbf{B}_e^2\cdot\mathbf{I})\mathbf{I}\}\right]\cdot\mathbf{D} + \frac{\partial g_d}{\partial\theta}\dot{\theta}, \tag{A1g}$$

$$\bar{g}_{d1} = -\left[\left\{\frac{\partial g_d}{\partial \alpha_1}\mathbf{I} + 2\frac{\partial g_d}{\partial \alpha_2}\mathbf{B}_e\right\}\cdot\tilde{\mathbf{A}} + \frac{\partial g_d}{\partial K}K\right], \quad \bar{g}_{d2} = -\left[\frac{\partial g_c}{\partial \phi_u}\right]. \tag{A1h,i}$$

It follows with the help of eqns (22) and (28) that

$$\dot{q} = \hat{g} - \Gamma\bar{g}_1 - \Gamma_\phi\bar{g}_2, \tag{A2a}$$

$$\dot{q}_c = \hat{g}_c - \Gamma\bar{g}_{c1} - \Gamma_\phi\bar{g}_{c2}, \tag{A2b}$$

$$\dot{q}_d = \hat{g}_d - \Gamma\bar{g}_{d1} - \Gamma_\phi\bar{g}_{d2}. \tag{A2c}$$

Now the loading and unloading behavior may be summarized by the following six cases:

Elastic response

$$\begin{aligned} &g < 0 \quad \text{or} \quad g = 0 \quad \text{and} \quad \hat{g} \leqslant 0, \quad \text{and} \\ &g_c < 0 \quad \text{or} \quad g_c = 0 \quad \text{and} \quad \hat{g}_c \leqslant 0, \quad \text{and} \\ &g_c < 0 \quad \text{or} \quad g_d = 0 \quad \text{and} \quad \hat{g}_d \leqslant 0, \end{aligned} \tag{A3a}$$

$$\Gamma = 0, \quad \Gamma_\phi = 0. \tag{A3b,c}$$

Plastic distortional deformation without compaction or dilation

$$g = 0 \quad \text{and} \quad \dot{g} > 0, \quad \text{and}$$
$$g_c < 0 \quad \text{or} \quad g_c = 0 \quad \text{and} \quad \dot{g}_{c1} \leqslant 0, \quad \text{and}$$
$$g_d < 0 \quad \text{or} \quad g_d = 0 \quad \text{and} \quad \dot{g}_{d1} \leqslant 0, \tag{A4a}$$

$$\dot{q}_{c1} = \dot{q}_c - (\dot{q}\ \bar{q}_1)\bar{q}_{c1}, \quad \dot{q}_{d1} = \dot{q}_d - (\dot{q}\ \bar{q}_1)\bar{q}_{d1}, \tag{A4b,c}$$

$$\Gamma = \dot{q}\ \bar{q}_1, \quad \Gamma_\phi = 0. \tag{A4d,e}$$

Porous compaction without plastic distortional deformation

$$g < 0 \quad \text{or} \quad g = 0 \quad \text{and} \quad \dot{g}_2 \leqslant 0, \quad \text{and} \quad g_c = 0 \quad \text{and} \quad \dot{g}_c > 0, \tag{A5a}$$

$$\dot{q}_2 = \dot{q} - (\dot{q}_c\ \bar{q}_{c2})\bar{q}_{c2}, \tag{A5b}$$

$$\Gamma = 0, \quad \Gamma_\phi = \dot{q}_c\ \bar{q}_{c2}. \tag{A5c,d}$$

Porous dilation without plastic distortional deformation

$$g < 0 \quad \text{or} \quad g = 0 \quad \text{and} \quad \dot{g}_2 \leqslant 0, \quad \text{and} \quad g_d = 0 \quad \text{and} \quad \dot{g}_d > 0, \tag{A6a}$$

$$\dot{q}_2 = \dot{q} - (\dot{q}_d\ \bar{q}_{d2})\bar{q}_{d2}, \tag{A6b}$$

$$\Gamma = 0, \quad \Gamma_\phi = \dot{q}_d\ \bar{q}_{d2}. \tag{A6c,d}$$

Porous compaction with plastic distortional deformation

$$g = 0 \quad \text{and} \quad \dot{g}_2 > 0, \quad \text{and} \quad g_c = 0 \quad \text{and} \quad \dot{g}_{c1} > 0, \tag{A7a}$$

$$\dot{q}_2 = \dot{q} - (\dot{q}_c\ \bar{q}_{c2})\bar{q}_{c2}, \quad \dot{q}_{c1} = \dot{q}_c - (\dot{q}\ \bar{q}_1)\bar{q}_{c1}, \tag{A7b,c}$$

$$\Gamma = \frac{\bar{q}_{c2}\dot{q}_2}{\bar{q}_1\bar{q}_{c2} - \bar{q}_2\bar{q}_{c1}}, \quad \Gamma_\phi = -\frac{\bar{q}_1\dot{q}_{c1}}{\bar{q}_1\bar{q}_{c2} - \bar{q}_2\bar{q}_{c1}}. \tag{A7d,e}$$

Porous dilation with plastic distortional deformation

$$g = 0 \quad \text{and} \quad \dot{g}_2 > 0, \quad \text{and} \quad g_d = 0 \quad \text{and} \quad \dot{g}_{d1} > 0, \tag{A8a}$$

$$\dot{q}_2 = \dot{q} - (\dot{q}_d\ \bar{q}_{d2})\bar{q}_{d2}, \quad \dot{q}_{d1} = \dot{q}_d - (\dot{q}\ \bar{q}_1)\bar{q}_{d1}, \tag{A8b,c}$$

$$\Gamma = \frac{\bar{q}_{d2}\dot{q}_2}{\bar{q}_1\bar{q}_{d2} - \bar{q}_2\bar{q}_{d1}}, \quad \Gamma_\phi = -\frac{\bar{q}_1\dot{q}_{d1}}{\bar{q}_1\bar{q}_{d2} - \bar{q}_2\bar{q}_{d1}}. \tag{A8d,e}$$

In the above, it has been assumed that porous compaction and dilation are mutually exclusive processes. Notice that: eqns (A7) reduce to eqns (A5) when $\dot{q}_2$ vanishes; eqns (A7) reduce to eqns (A4) when $\dot{q}_{c1}$ vanishes; eqns (A8) reduce to eqns (A6) when $\dot{q}_2$ vanishes; and eqns (A8) reduce to eqns (A4) when $\dot{q}_{d1}$ vanishes. This means that there is a smooth transition from cases where two yield surfaces are active to cases where only one yield surface is active. Furthermore, it is noted that the constitutive equations for the yield surfaces must be restricted so that

$$\bar{q}_1 > 0 \quad \text{for Case (A4)}. \tag{A9a}$$

$$\bar{q}_{c2} > 0 \quad \text{for Case (A5)}. \tag{A9b}$$

$$\bar{q}_{d2} > 0 \quad \text{for Case (A6)}. \tag{A9c}$$

$$\Gamma \geqslant 0, \Gamma_\phi \geqslant 0, (\bar{q}_1\bar{q}_{c2} - \bar{q}_2\bar{q}_{c1}) \neq 0 \quad \text{for Case (A7)}. \tag{A9d}$$

$$\Gamma \geqslant 0, \Gamma_\phi \geqslant 0, (\bar{q}_1\bar{q}_{d2} - \bar{q}_2\bar{q}_{d1}) \neq 0 \quad \text{for Case (A8)}. \tag{A9e}$$

Finally, it is mentioned that with the help of eqns (A2), it follows that: eqns (A4) satisfy the consistency condition $\dot{g} = 0$; eqns (A5) satisfy the consistency condition $\dot{g}_c = 0$; eqns (A6) satisfy the consistency condition $\dot{g}_d = 0$; eqns (A7) satisfy the consistency conditions $\dot{g} = 0$, $\dot{g}_c = 0$; and eqns (A8) satisfy the consistency conditions $\dot{g} = 0$, $\dot{g}_d = 0$.